Study of the Low-Lying Levels of F^{18} by Means of the $O^{16}(He^3,p\gamma)F^{18}$ Reaction

A. R. POLETTI AND E. K. WARBURTON*
Nuclear Physics Laboratory, Oxford, England
(Received 21 September 1964)

The particle-gamma angular-correlation method of Litherland and Ferguson was used to gain information on the decay modes and spin assignments of the first ten excited states of F^{18}. The $O^{16}(He^3,p)F^{18}$ reaction was used with He^3 energies between 3.0 and 4.2 MeV. Protons were detected in an annular counter at 180° to the beam and gamma rays were detected at angles between 0° and 90° to the beam. Decay modes are given for all ten states of F^{18} below 3.5-MeV excitation. Spin assignments of (0,1,2), 1, (1,2), 2, 1, and (2,3) were established for the levels at 1.08, 1.70, 2.10, 2.53, 3.13, and 3.35 MeV. The present results combined with previous work lead to an assignment of 3^+ for the 0.940-MeV level, a most probable assignment of 2 for the 3.06-MeV level, and 2^+ for the 2.53-MeV level. Dipole-quadrupole or quadrupole-octupole mixing ratios were obtained for some of the gamma-ray transitions. The results are compared with previous shell-model predictions.

I. INTRODUCTION

THERE has been considerable theoretical interest over the past ten years in the energy level structure of the O^{18}-F^{18}-Ne^{18} triad of nuclei.[1–7] As a result, there exists a considerable body of theoretical predictions for the excitation energies and characteristics of the bound levels of O^{18} and F^{18}. On the experimental side, the $T=1$ spectrum of levels in O^{18} has been studied extensively and the energy positions, spins, and parities of the levels below an excitation energy of 4 MeV have been determined.[8] The experimental information concerning the $T=0$ spectrum in F^{18} is much less complete. The excitation energies of 17 energy levels below the α-particle binding energy of 4.421 MeV in F^{18} have been determined[8] accurately (±10 keV), but as recently as 1962 definite spin, parity, and isotopic-spin assignments had been made to only two of these levels.[8] This lack of information on the characteristics of the bound levels of F^{18} is, at the present time, the main deterrent to a thorough testing of the theoretical[1–7] predictions for the mass-18 system.

The available information on the energy levels of F^{18} below 3.5-MeV excitation is shown in Table I. The information given in this table is taken mainly from the compilations of Ajzenberg-Selove and Lauritsen.[8] References are also given to recent work.[9–15] Uncertain spin-parity and isotopic-spin assignments are enclosed in parentheses. The isotopic-spin assignments are based on the $Ne^{20}(d,\alpha)F^{18}$ work of Freeman[16] and on the spectrum of $T=1$ states in O^{18}. The tentative even-parity assignment for the 2.53-MeV level and the tentative spin-parity assignments for the 3.35-MeV level are based on results of the $F^{19}(d,t)F^{18}$ reaction[13] and the $F^{19}(p,d)F^{18}$ reaction.[15]

This paper describes a study of the lowest ten excited levels of F^{18} by the measurement of proton-gamma (p,γ) correlations following the excitation of the levels by the $O^{16}(He^3,p)F^{18}$ reaction ($Q=2.021$ MeV). These (p,γ) measurements lead to determinations of branch-

TABLE I. Available information on the energy levels of F^{18}.

Energy (MeV) (±10 keV)	$J^\pi; T$	Mean lifetime (sec)	Reference
0	$1^+; 0$		
0.940	$2, 3^+; 0$	$2\times10^{-10}>\tau>3\times10^{-12}$	9, 10
1.045	$0^+; 1$	$\tau<3\times10^{-13}$	10
1.082	$\leq 3; 0$	$2\times10^{-8}\geq\tau>10^{-12}$	10, 11
1.125	$(5)^+; 0$	$(1.9\pm0.5)\times10^{-7}$	12
1.700	$1^+; 0$	$(2\pm1)\times10^{-12}$	10
2.104	$1, 2, 3; 0$	$(0.7\pm0.2)\times10^{-12}$	10
2.525	$1^{(+)}, 2^{(+)}$ $3^{(+)}; 0$	$(1.1\pm0.2)\times10^{-12}$	10, 13
3.063	$(2^+; 1)$		14
3.133	$?; (0)$		14
3.354	$(0^-, 1^-, 2^-); 0$		13, 15

* National Science Foundation senior postdoctoral fellow, 1963–1964. Permanent address: Brookhaven National Laboratory, Upton, New York.

[1] M. G. Redlich, Phys. Rev. **95**, 448 (1954); Phys. Rev. **99**, 1427 (1955).
[2] J. P. Elliott and B. H. Flowers, Proc. Roy. Soc. (London) **A229**, 536 (1955).
[3] M. G. Redlich, Phys. Rev. **110**, 468 (1958).
[4] T. Inoue, T. Sebe, H. Hagiwara, and A. Arima, Nucl. Phys. **59**, 1 (1964).
[5] B. H. Flowers and D. Wilmore, Proc. Phys. Soc. (London) **83**, 683 (1964).
[6] J. F. Dawson, I. Talmi, and J. D. Walecka, Ann. Phys. (N. Y.) **18**, 339 (1962).
[7] M. Harvey, Phys. Letters **3**, 209 (1963).
[8] F. Ajzenberg-Selove and T. Lauritsen, Nucl. Phys. **11**, 1 (1959); T. Lauritsen and F. Ajzenberg-Selove, Nuclear Data Sheets, compiled by K. Way *et al.* [Printing & Publishing Office, National Academy of Sciences–National Research Council, Washington 25, D. C. 1962. NRC 61-Sets 5, 6 (339 pp.)].
[9] J. Lowe and C. L. McClelland, Phys. Rev. **132**, 367 (1963).
[10] A. E. Litherland, M. J. Yates, B. M. Hinds, and D. Eccleshall, Nucl Phys. **44**, 220 (1963).
[11] J. A. Kuehner, E. Almqvist, and D. A. Bromley, Phys. Rev. **122**, 908 (1961).
[12] K. W. Allen, D. Eccleshall, and M. J. L. Yates, Proc. Phys. Soc. (London) **74**, 660 (1959).
[13] N. A. Vlasov, S. P. Kalinin, A. A. Ogoblin, and V. I. Chuev, Zh. Eksperim. i Teor. Fiz. **37**, 1187 (1959) [English transl.: Soviet Physics—JETP **10**, 844 (1960)].
[14] G. M. Matous and C. P. Browne, Bull. Am. Phys. Soc. **9**, 69 (1964); Phys. Rev. **136**, B399 (1964).
[15] E. F. Bennett, Phys. Rev. **122**, 595 (1961).
[16] J. Freeman (private communication), also quoted in Ref. 11.

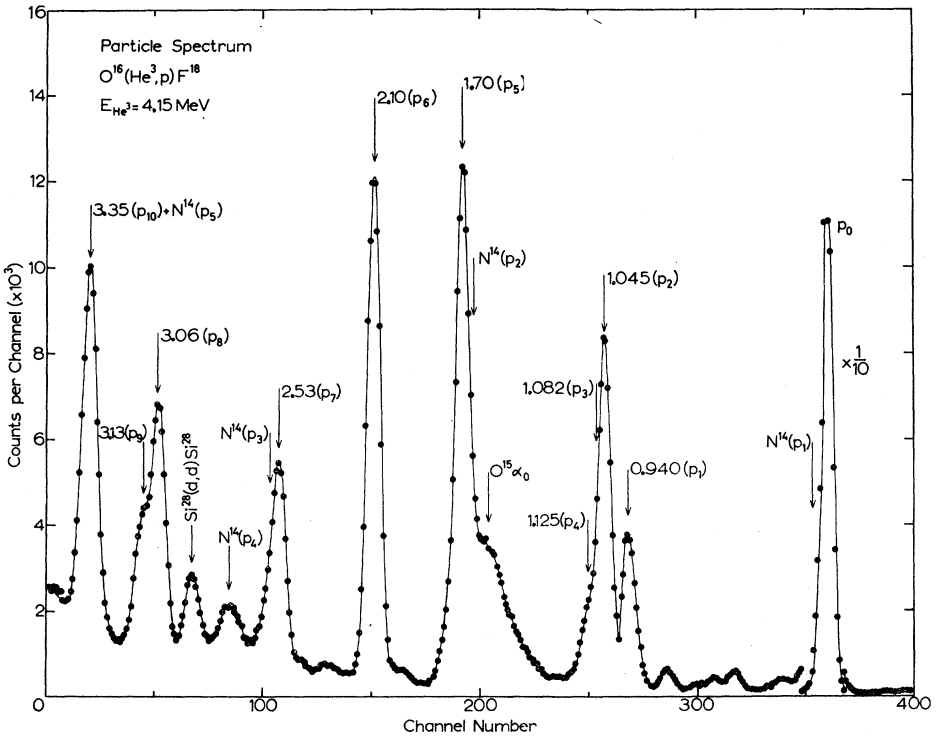

FIG. 1. Particle spectrum in the 180° annular counter from bombardment of a 50 μg/cm^2 SiO target with a 4.15-MeV He^3 beam and a 3.4 mg/cm^2 aluminum foil in front of the counter. The F^{18} proton peaks are identified by the excitation energies and sequence of the levels to which they correspond. The N^{14} proton peaks, which arise from $C^{12}(He^3,p)N^{14}$, are so labeled. The ground-state alpha group from $O^{16}(He^3,\alpha)O^{15}$ and the deuteron group from $Si^{28}(d,d)Si^{28}$ are also indicated.

ing ratios and mixing parameters for the de-excitation gamma rays and to information on the spin assignments of these levels. The experimental method and the method of theoretical analysis which is used was developed by Litherland and Ferguson.[17] Basically the method is one of limiting the population of an excited level to a few magnetic substates, thereby imposing constraints on the angular distributions of the de-excitation gamma rays. Since these constraints are dependent on the spin of the emitting state and the mixing parameters of the gamma rays, analysis of the gamma-ray angular distributions yields possible sets of these parameters which are quite often found to be unique. The limitation on the population of the magnetic substates is imposed by detecting the emitted particles h_2 in a nuclear reaction $X(h_1,h_2)Y^*$ in an axially symmetrical counter at 0° or 180° to the beam following absorption of the unpolarized particles h_1 in the direction of the quantization axis. With this condition only those magnetic substates of Y^* will be formed which have magnetic quantum numbers α equal to or less than the sum of the spins of X, h_1, and h_2. There is also the general restriction for unpolarized beams, $P(\alpha)=P(-\alpha)$, where $P(\alpha)$ is the population number of the substate with magnetic quantum number α.[17] Some specific examples of the use of this method are particle-gamma correlations in the $Mg^{26}(He^4,n\gamma)Si^{29}$ reaction,[18] the $F^{19}(He^4,p\gamma)Ne^{22}$ reaction,[19] and the $S^{32}(p,p'\gamma)S^{32}$ and $Ca^{40}(p,p'\gamma)Ca^{40}$ reactions.[20]

A previous extensive study of the $O^{16}(He^3,p\gamma)F^{18}$ reaction has been reported by Kuehner, Almqvist, and Bromley.[11] These measurements were not obtained or analyzed using the method of Litherland and Ferguson.[17]

II. EXPERIMENTAL PROCEDURE

The experiments were performed using He^3 ions with energies between 3.0 and 4.2 MeV from the Harwell Van de Graaff generator. The analyzed beam of about 0.2 μA entered the target chamber through a collimating system which consisted of five tantalum collimators with a lead cylinder between each one. It had a total length of 45 cm. The first four collimators were 2.4 mm in diameter while the last one, an antiscatterer, was 3.2 mm in diameter. The lead cylinders were each 9 cm long with a 6.4-mm central hole. A lead cylinder of the same dimensions also followed the antiscattering collimator which was itself 65 cm from the target.

The target chamber was essentially a 15.24-cm-diam brass cylinder with a 1.6 mm thick wall.

The targets were self-supporting films of SiO which were made by vacuum evaporation of SiO from a tantalum boat on to a glass slide, which had previously been lightly smeared with a commercial detergent. The films were floated off the glass slide on hot water prior to

[17] A. E. Litherland and A. J. Ferguson, Can. J. Phys. **39**, 788 (1961).
[18] A. E. Litherland and G. J. McCallum, Can. J. Phys. **38**, 927 (1960).
[19] D. Pelte, B. Povh, and W. Scholz, Nucl. Phys. **52**, 333 (1964).
[20] A. R. Poletti and M. A. Grace (to be published).

mounting on the target frames. The experiments were done in two series. In the first the target thickness was 180 μg/cm^2 and in the second it was 50 μg/cm^2. The energy losses for 4-MeV He^3 ions in these targets were 120 and 35 keV, respectively.

After passing through the target the beam was stopped in a copper beam catcher which was 3.6 m from the target in the first series of measurements and 12.7 cm from the target in the second.

The charged particle spectrum from the target was detected by a silicon semiconductor counter at 180° to the He^3 beam and 4.0 cm from the target. This detector was made from a disk of 6500 $\Omega\cdot$cm n-type silicon 1 mm thick by 20 mm diameter with a 6.3-mm-diam hole in the center through which the He^3 beam passed. The sensitive area was an annular ring of 4 mm width and 9 mm inner diameter. The inner and outer edges of the sensitive area subtended angles at the target center of 172° and 168°, respectively. The counter stopped ~5-MeV protons with a bias of 80 V and had an intrinsic resolution of 50 keV. Elastically scattered He^3 particles were stopped and α particles from the $O^{16}(He^3,\alpha)O^{15}$ reaction were degraded by an aluminium foil placed in front of the proton counter. In the first series of measurements the foil was 6.7 mg/cm^2 thick, while in the second it was 3.4 mg/cm^2 thick. The width of the proton groups was largely determined by the thickness of the target and the energy spread in these foils. A proton spectrum recorded in the second series of measurements with a 4.15-MeV He^3 beam is shown in Fig. 1, while a proton spectrum recorded in the first series with a 3.75-MeV He^3 beam is shown in Fig. 2.

The expected positions of the proton groups due to the F^{18} ground state and all ten of the F^{18} excited states below an excitation energy of 3.5 MeV are indicated in Fig. 1. The expected positions of the proton groups corresponding to the first five excited states[8] of N^{14} produced by the $C^{12}(He^3,p)N^{14}$ reaction (Q=4.78 MeV) are also shown. The $N^{14}(p_4)$ group (corresponding to the 5.10-MeV level) at channel 85 is the only one of these which is clearly resolved in Fig. 1. None of the N^{14} groups are discernible in Fig. 2. Carbon contamination of the SiO target was a source of difficulty in the study of the decays of the F^{18} 2.53- and 3.35-MeV levels but not in any other case. Two other peaks identified in Fig. 1 are the ground state α group from $O^{16}(He^3,\alpha)O^{15}$, and the group due to elastic scattering of deuterons on Si^{28}. The α group does not appear in Fig. 2 because of the thicker foil used, while the deuteron group was produced by a small contamination of the He^3 beam by HD^+, for which the momentum/charge ratio is almost identical to that for the singly-charged He^3 beam.

The other small peaks in the spectrum of Fig. 1 were not identified. Presumably at least some of them are due to the reaction $Si^{28}(He^3,p)P^{30}$ (Q=6.34 MeV). If so the proton groups from this reaction in the region shown in Fig. 1 are due to levels in P^{30} with excitation energies greater than 4 MeV. No gamma rays were observed in this work from any reactions other than $O^{16}+He^3$ and $C^{12}+He^3$.

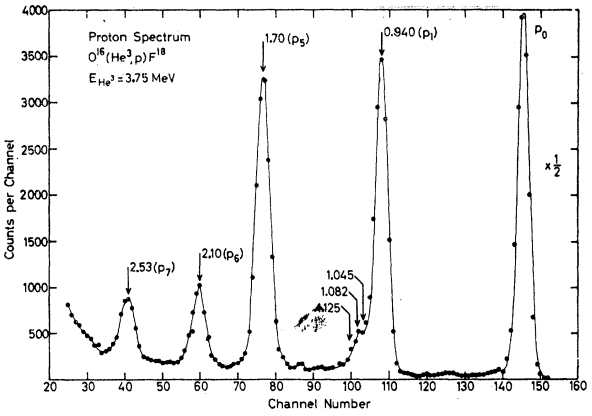

FIG. 2. Proton spectrum in the 180° annular counter from bombardment of a 180 μg/cm^2 SiO target with a 3.75-MeV He^3 beam and a 6.7 mg/cm^2 aluminum foil in front of the counter. The proton peaks are identified by the excitation energies of the levels to which they correspond.

The gamma-ray detectors were NaI(Tl) crystals. A 7.6 cm×7.6 cm crystal, with its front face 15 cm from the target, was used in the first series of runs, while in the second series a crystal 12.7 cm diameter by 15.2 cm long was used with its front face 25 cm from the target. Their resolutions for gamma rays of 2.62 MeV were 5.9% and 6.4% full width at half-maximum, respectively. The detectors were mounted on a trolley which rotated about the central vertical axis of the correlation table. The center of the target was checked by measurement to be within ±1 mm of this central axis. The intrinsic isotropy of the system was checked in two ways: (1) by placing a radioactive source in the target position and counting at each angle for a fixed time, (2) by (p,γ) correlation experiments on the gamma rays de-exciting the $J^\pi=0^+$, F^{18} 1.04-MeV level.

For angles between 20° and 90° the first method showed that the counting rate remained constant to within 1%; while the second method indicated isotropy to within the statistical errors which were approximately ±5%. In the second series of measurements the correlations were extended to 0°. At this angle the NaI(Tl) crystal was partly obscured by a small flange of the scattering chamber. The attenuation due to this cause was determined at the same time as the isotropy was checked. This fixed the attenuation for gamma rays of 1.04 and 2.62 MeV. A correlation on the $J=1$ level at 1.70 MeV gave the attenuation for gamma rays of 0.66 MeV, since the distribution could be accurately extrapolated to 0° (See Sec. IVA). The gain of the gamma-ray amplifier and photomultiplier was kept constant by the use of gain stabilization. Either a "Spectrastat"[21] was used for this or else a system which stabilized upon receiving pulses from a pulsed light source.[22]

[21] Commercially available from Cosmic Radiation Labs., Inc., Bellport, New York.

[22] J. L. Black and E. Valentine (private communication).

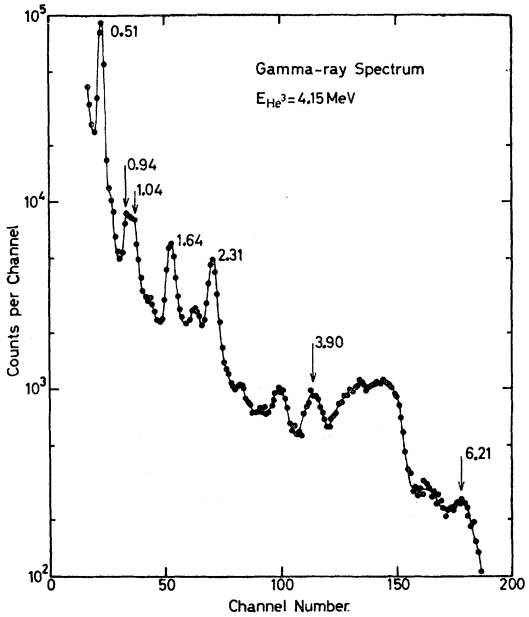

FIG. 3. Gamma-ray spectrum from bombardment of a 50 μg/cm^2 SiO target with a 4.15-MeV He^3 beam observed using a 12.7-cm-diam by 15.2-cm-long NaI(Tl) crystal. The majority of the gamma rays are from $C^{12}+He^3$ reactions and originate in the collimating and beam-stopping system.

The gamma-ray singles spectra were dominated by N^{14} de-excitation gamma rays from the $C^{12}(He^3,p)N^{14}$ reaction. This is illustrated in Fig. 3 which shows a singles spectrum recorded at $E_{He^3}=4.0$ MeV using the 12.7-cm-diam by 15.2-cm-long NaI(Tl) crystal at 45° to the beam. The 0.94- and 1.04-MeV peaks shown in Fig. 3 are due to the ground state decays of the first and second excited states of F^{18}. These two peaks are the only ones discernible in Fig. 3 which arise from $O^{16}+He^3$. Apart from these two F^{18} peaks, the spectrum shown in Fig. 3 is characteristic of $C^{12}+He^3$ gamma rays.[23] The vast majority of these $C^{12}+He^3$ gamma rays originated in the collimating and beam-stopping system. However, as is clear from Fig. 1, a small fraction arise from carbon contamination of the SiO target.

A single-channel analyzer selected pulses corresponding to the proton group to be studied. Coincidences were then determined between these selected pulses and all pulses from the gamma-ray detector. Two standard slow coincidence boxes were used in parallel: one whose delay was set at the correct value to obtain true coincidences, and a second which sampled the random coincidences. Gamma-ray pulses corresponding to coincidences in the different boxes were routed into separate halves of the multichannel analyzer used to record the coincidence spectra. The resolving times used were 0.2 or 0.1 μsec. This gave a ratio of real to random coincidences (integrated over the whole spectrum) of between 6:1 and 3:1. From Fig. 3 it can be seen that most of these occur in the 0.51-MeV annihilation peak or at lower energies, so that the random coincidence counts underlying the peaks of interest were generally less than 10% of the real coincidences. The total charge delivered by the beam was monitored by a current integrator with an accuracy of 0.1%. Also, the total number of counts from the proton counter, the gamma-ray detector, and the single-channel analyzer were recorded. Consequently any instability of the apparatus, or changes in the target, could quickly be detected.

The number of angles at which measurements are taken depends upon the expected complexity of the distribution being measured. Transitions involving $L\geq 3$ were not expected in this work; hence the most complex correlation which would have been encountered is one in which terms in $P_4(\cos\theta)$ were present, i.e., for a given correlation at least three experimental points would have been required. Measurements in most cases were actually taken at five points, at least two of which were repeated to check on reproducibility.

III. THEORY

A. The General Gamma-Ray Distribution Formula

In this subsection we present a form of the general gamma-ray distribution formula which is particularly suitable for use with the Litherland–Ferguson method,[17] or, more generally, for the interpretation of gamma-ray angular distributions relative to any quantization axis possessing rotational symmetry.

We are concerned with the emission of gamma radiation from an aligned nuclear state with spin a. The alignment could be achieved by a nuclear reaction of the type $X(h_1,h_2)Y^*$, by resonant or nonresonant particle capture, or by methods other than nuclear reactions. The nuclear state is assumed to have a well-defined parity and to be unpolarized, i.e., the magnetic substates are assumed to be symmetrically populated. If the nuclear state is formed by a nuclear reaction, then the quantization axis will usually be the beam axis. This is true in the case of particle capture or $X(h_1,h_2)Y^*$ reactions with h_2 unobserved as well as for the present application where h_2 is detected in a counter axially symmetric about the beam direction. However, the quantization axis is not necessarily the beam axis. An example is the case where the reaction $X(h_1,h_2)Y^*$ is a direct interaction described by the plane wave Born approximation. In this case, if the particles h_2 are detected in a specific direction an axis of rotational symmetry can be defined in the direction of recoil of Y^*.

We consider first the case where the state with spin a (magnetic quantum numbers α) decays by gamma emission to a state with spin b. Then the angular distribution of the gamma rays can be expressed by

$$W(\theta_1)=\sum_k a_k P_k(\cos\theta_1)=\sum_k \rho_k(a)F_k(ab)Q_k P_k(\cos\theta_1)\,, \quad (1)$$

[23] E. K. Warburton, J. W. Olness, D. E. Alburger, D. J. Bredin, and L. F. Chase, Jr., Phys. Rev. 134, B338 (1964).

TABLE II. Statistical tensor coefficients, $\rho_k(a,\alpha)$ for $a=1$ to 6.

a	k	α 0	1	2	3	4	5	6
1	2	−1.4142	1.4142					
2	2	−1.1952	−1.1952	2.3904				
	4	1.6036	−2.1381	0.5345				
3	2	−1.1547	−1.7321	0.0000	2.8868			
	4	1.2792	0.4264	−2.9848	1.2792			
	6	−1.7408	2.6112	−1.0445	0.1741			
4	2	−1.1396	−1.9373	−0.9117	0.7977	3.1909		
	4	1.2069	1.2069	−1.4751	−2.8160	1.8774		
	6	−1.3484	0.1348	2.9665	−2.2923	0.5394		
	8	1.8511	−2.9618	1.4809	−0.4232	0.0529		
5	2	−1.1323	−2.0381	−1.3587	−0.2265	1.3587	3.3968	
	4	1.1767	1.5689	−0.3922	−2.3534	−2.3534	2.3534	
	6	−1.2524	−0.7515	2.2544	1.8161	−3.0059	0.9393	
	8	1.4085	−0.5634	−2.7365	2.9377	−1.2475	0.2013	
	10	−1.9445	3.2408	−1.8519	0.6944	−0.1544	0.0154	
6	2	−1.1282	−2.0951	−1.6117	−0.8058	0.3223	1.7728	3.5457
	4	1.1609	1.7689	0.3040	−1.4925	−2.6534	−1.8242	2.7363
	6	−1.2098	−1.2098	1.3308	2.6010	0.4839	−3.3267	1.3308
	8	1.2941	0.3697	−2.6252	−0.7026	3.2907	−2.0335	0.4067
	10	−1.4619	0.9050	2.4364	−3.3066	1.9260	−0.5685	0.0696
	12	2.0259	−3.4731	2.1707	−0.9648	0.2894	−0.0526	0.0044

where θ_1 is the angle between the direction of emission of the gamma rays and the axis of alignment. In Eq. (1), $P_k(\cos\theta_1)$ is a Legendre polynomial and k takes on even values from 0 to $2a$. The Q_k are attenuation coefficients[17] for the gamma-ray detector, the $\rho_k(a)$ are statistical tensors which describe the alignment of the initial state, and the $F_k(ab)$ depend specifically on the gamma-ray cascade and, most importantly, are independent of the nuclear alignment.[24]

The statistical tensors $\rho_k(a)$ are given by a weighted sum over the population parameters of the $2a+1$ magnetic substates associated with a, i.e.,

$$\rho_k(a)=\sum_\alpha \rho_k(a,\alpha)P(\alpha)\,. \tag{2}$$

The state a is unpolarized so that $P(\alpha)=P(-\alpha)$. The normalization is such that $\sum_\alpha P(\alpha)=1$, so that the $P(\alpha)$ are in the range $0\leq P(\alpha)\leq\frac{1}{2}(1+\delta_{\alpha 0})$. We chose to limit the sum in Eq. (2) to $\alpha\geq 0$, with the result

$$\rho_k(a,\alpha)=(2-\delta_{\alpha 0})\frac{(a\alpha a-\alpha|k0)}{(a\alpha a-\alpha|00)}\,. \tag{3}$$

A consequence of Eq. (3) is that $\rho_k(a,\alpha)=\rho_k(a,-\alpha)$. Obviously $\rho_0(a,\alpha)=(2-\delta_{\alpha 0})$ so that[25] $\rho_0(a)=1$. The $\rho_k(a,\alpha)$ for integer values of a between 1 and 6 are listed in Table II, while those for half-integer values of a between 3/2 and 11/2 are listed in Table III.

The $F_k(ab)$ are given in general by

$$F_k(ab)=\sum_{LL'} i^{L'-L+\pi-\pi'}x_L x_{L'}F_k(LL'ba)/\sum_L x_L^2\,, \tag{4}$$

where the sum is over all integer values of L and L' from $|a-b|$ to $a+b$ (with the obvious restriction $L,L'\neq 0$), π and π' are associated with L and L', respectively, π is 0 for electric and 1 for magnetic radiation. The sign convention is that of Litherland and Ferguson.[17] The x_L and $x_{L'}$ are given by ratios of reduced matrix elements:

$$x_L=\frac{\langle b||L||a\rangle}{\langle b||L_m||a\rangle};\quad x_{L'}=\frac{\langle b||L'||a\rangle}{\langle b||L_m||a\rangle}\,. \tag{5}$$

The reduced matrix elements are real and L_m is the lowest allowed value of L, i.e., $L_m=1$ for $a=b$ and $L_m=|a-b|$ otherwise. The $F_k(LL'ba)$, which are given by

$$F_k(LL'ba)=(-)^{b-a-1}[(2L+1)(2L'+1)(2a+1)]^{1/2}\times(L1L'-1|k0)W(aaLL',kb)\,, \tag{6}$$

have the symmetry $F_k(LL'ba)=F_k(L'Lba)$, and the normalization $F_0(LL'ba)=\delta_{LL'}$. The triangular conditions on the Racah coefficient in Eq. (6) limit k to $k\leq\min(2L,2L',2a)$. The $F_k(LL'ba)$ have been tabulated[26] in decimal form for a and b up to 12 and a large range of values of L and L'. The form adopted here for the angular distribution formula was chosen in order to take advantage of this tabulation.

[24] We chose to normalize the factors appearing on the right of Eq. (1) so that $a_0\equiv\rho_0(a)F_0(ab)Q_0=1$. Equation (1) is identical to Eq. (23) of Ref. 17. It is felt that the form given here makes tabulation and hand calculation of the required coefficients easier. The $\rho_k(a)$ defined by Eqs. (2) and (3) are identical to $(2a+1)^{1/2}\rho_{k0}(a,a)$ where $\rho_{k0}(a,a)$ is defined by Eq. (3) of Ref. 17.

[25] The sum in Eq. (2) could just as well have been extended from $-a$ to a. In this case the factor $(2-\delta_{\alpha,0})$ would have been omitted from Eq. (3) and $\rho_k(a)$ would have remained unchanged.

[26] M. Ferentz and N. Rosenzweig, Argonne National Laboratory Report ANL 5324 (unpublished). Other tabulations of these functions are referred to in this report.

TABLE III. Statistical tensor coefficients, $\rho_k(a,\alpha)$ for $a=\frac{3}{2}$ to 11/2.

		α					
a	k	$\frac{1}{2}$	$\frac{3}{2}$	$\frac{5}{2}$	$\frac{7}{2}$	$\frac{9}{2}$	11/2
$\frac{3}{2}$	2	−2.0000	2.0000				
$\frac{5}{2}$	2	−2.1381	−0.5345	2.6726			
	4	1.8516	−2.7774	0.9258			
$\frac{7}{2}$	2	−2.1822	−1.3093	0.4364	3.0551		
	4	2.0513	−0.6838	−2.9630	1.5954		
	6	−1.7408	3.1334	−1.7408	0.3482		
$\frac{9}{2}$	2	−2.2020	−1.6515	−0.5505	1.1010	3.3030	
	4	2.1288	0.3548	−2.0105	−2.6019	2.1288	
	6	−1.9694	1.4771	2.4618	−2.7079	0.7385	
	8	1.6557	−3.3113	2.3652	−0.8278	0.1183	
11/2	2	−2.2124	−1.8331	−1.0746	0.0632	1.5803	3.4767
	4	2.1678	0.9290	−1.0065	−2.5549	−2.0904	2.5549
	6	−2.0684	0.4137	2.5855	1.1376	−3.2060	1.1376
	8	1.8992	−2.0077	−1.7635	3.2286	−1.6551	0.2985
	10	−1.5878	3.4024	−2.8353	1.3232	−0.3403	0.0378

The angular distribution of the second gamma ray (first gamma ray unobserved) in a cascade $a \rightarrow b \rightarrow c$ is given by[27]

$$W(\theta_2)=\sum_k \rho_k(a)U_k(ab)F_k(bc)Q_kP_k(\cos\theta_2)\,, \quad (7)$$

where

$$U_k(ab)=\sum_L x_L^2U_k(Lab)/\sum_L x_L^2. \quad (8)$$

Note that there are no interference terms between different multipolarities in Eq. (8). The $U_k(Lab)$ are given by

$$U_k(Lab)=\frac{W(abab;Lk)}{W(abab;L0)} \quad (9)$$

so that $U_0(Lab)=1$ and $U_k(Lab)=U_k(Lba)$. An expression for the angular distribution of the nth gamma ray in a cascade can be obtained by a generalization of Eq. (7). The result is

$$W(\theta_n)=\sum_k \rho_k(a)U_k(ab)U_k(bc)\cdots U_k(xy)F_k(yz) \times Q_kP_k(\cos\theta_n)\,, \quad (10)$$

where the sum in Eq. (10) contains the product of $n-1$ U_k coefficients

In practice it is usually sufficient to include only the two lowest allowed multipolarities in Eq. (4) and (8). This is assumed to be true in the present work on F^{18}. In this case Eqs. (4) and (8) become

$$F_k(ab)=\frac{F_k(LLba)-(-)^\sigma 2xF_k(LL'ba)+x^2F_k(L'L'ba)}{1+x^2} \quad (11)$$

and

$$U_k(ab)=\frac{U_k(Lab)+x^2U_k(L'ab)}{1+x^2}\,, \quad (12)$$

where now L is the lowest allowed value, and $L'=L+1$. In Eqs. (11) and (12) the mixing parameter x is given by $x=\langle b||L+1||a\rangle/\langle b||L||a\rangle$ so that the x_L and $x_{L'}$ of Eq. (5) have become $x_L\equiv 1$, $x_{L'}\equiv x$. In Eq. (11), σ is 0 for an ML, $EL+1$ mixture, and 1 for an EL, $ML+1$ mixture. This is the sign convention of Litherland and Ferguson.[17] In this report we shall always take $\sigma=0$ regardless of the known or suspected nature of the transition.

In Table IV the $U_k(Lab)$ and $U_k(L'ab)$ are listed to four decimal places for a and b less than our equal to 6, $L\leq 3$, and $k\leq 8$. Table V gives a selection of the coefficients $F_k(LL'ba)$ for integer values of a and b. The coefficients are listed to four decimal places for $a,b\leq 6$ ($a\neq 0$) and $L\leq 3$. In Table VI a similar listing for half-integer values of a and b is given for $a,b\leq 11/2$ ($a\neq\frac{1}{2}$) and $L\leq 3$.

B. Method of Analysis

The method of analysis follows very closely the linear least-squares fitting procedure developed at Chalk River[28] and Utrecht[29] for use with method I of Litherland and Ferguson.[17]

In the $O^{16}(He^3,p)F^{18}$ reaction with the protons detected at 180° only the $\alpha=0$, $\alpha=\pm 1$ magnetic substates can be populated. Then, since we assume that at most two multipolarities contribute to any transition, the unknowns involved in the angular distribution of a single primary gamma transition are the mixing parameter x and the ratio of $P(0)$ to $P(1)$. That is, we

[27] S. Devons and L. J. B. Goldfarb, *Handbuch der Physik*, edited by S. Flügge (Springer-Verlag, Berlin, 1957), Vol. 42, p. 362.

[28] C. Broude and H. E. Gove, Ann. Phys. (N. Y.) **23**, 71 (1963).

[29] P. W. M. Glaudemans and P. M. Endt, Nucl. Phys. **42**, 367 (1963).

TABLE IV. Angular distribution coefficients $U_k(Lab)$ and $U_k(L+1ab)$ for $a,b\leq 6$ and $k\leq 8$.

		k							
		2		4		6		8	
a	b	L	$L+1$	L	$L+1$	L	$L+1$	L	$L+1$
1	1	−0.5000	0.1000						
	2	0.5916	−0.5916						
	3	0.4899	−0.6124						
	4	0.4432	−0.6205						
3/2	3/2	0.2000	−0.6000						
	5/2	0.7483	−0.1069						
	7/2	0.6547	−0.2182						
	9/2	0.6055	−0.2752						
2	2	0.5000	−0.2143	−0.6667	0.2857				
	3	0.8281	0.2070	0.4179	−0.6268				
	4	0.7492	0.0749	0.2847	−0.5694				
	5	0.7037	0.0000	0.2271	−0.5300				
5/2	5/2	0.6571	0.1000	−0.1429	−0.5000				
	7/2	0.8748	0.4082	0.5803	−0.4513				
	9/2	0.8092	0.2795	0.4349	−0.5140				
	11/2	0.7687	0.2010	0.3624	−0.5296				
3	3	0.7500	0.3167	0.1667	−0.5000	−0.7500	0.4167		
	4	0.9047	0.5428	0.6814	−0.2271	0.3228	−0.5809		
	5	0.8498	0.4249	0.5436	−0.3624	0.1853	−0.4633		
	6	0.8142	0.3489	0.4675	−0.4230	0.1308	−0.3924		
7/2	7/2	0.8095	0.4667	0.3651	−0.3333	−0.3333	−0.3333		
	9/2	0.9250	0.6366	0.7495	−0.0292	0.4714	−0.5571		
	11/2	0.8787	0.5311	0.6245	−0.1990	0.3060	−0.5415		
4	4	0.8500	0.5734	0.5000	−0.1494	−0.0500	−0.5136	−0.8000	0.5091
	5	0.9394	0.7045	0.7977	0.1330	0.5742	−0.4306	0.2629	−0.5257
	6	0.9000	0.6107	0.6861	−0.0490	0.4053	−0.5066	0.1300	−0.3715
9/2	9/2	0.8788	0.6515	0.5960	0.0152	0.1515	−0.4848	−0.4545	−0.1818
	11/2	0.9503	0.7551	0.8332	0.2635	0.6492	−0.2830	0.3963	−0.5792
5	5	0.9000	0.7103	0.6667	0.1538	0.3000	−0.3821	−0.2000	−0.4462
	6	0.9580	0.7938	0.8601	0.3686	0.7059	−0.1412	0.4947	−0.5230
11/2	11/2	0.9161	0.7554	0.7203	0.2687	0.4126	−0.2587	−0.0070	−0.5105
6	6	0.9286	0.7909	0.7619	0.3636	0.5000	−0.1364	0.1429	−0.4805

wish to fit the measured angular distributions for a transition between the states with spins a and b with the theoretical distribution [see Eqs. (1) and (2)].

$$W(\theta)=\sum_k [\rho_k(a,0)I(0)+\rho_k(a,1)I(1)]. F_k(a,b)Q_kP_k(\cos\theta), \quad (13)$$

where $4\pi I(0)$ and $4\pi I(1)$ are the total intensities for forming the magnetic substates $\alpha=0$ and $\alpha=1$, respectively, $I(0)$ and $I(1)$ are constrained to be positive or zero, and

$$P(0)=I(0)/[I(0)+2I(1)], P(1)=I(1)/[I(0)+2I(1)].$$

The problem is to determine $P(0)$, $P(1)$ and the mixing parameter x by a least-squares fit of Eq. (13) to the measured angular distribution for all allowed values of the spins a and b. If x is taken as a continuous variable, then the nonlinear method of least squares is appropriate and the problem must be solved by an iterative procedure.[28,29] To avoid this complication a linear least-squares fit of Eq. (13) to the measured distribution is made for a discrete set of fixed values of x. For each value of x the best fit corresponds to those values of $P(0)$ and $P(1)$ yielding the lowest value of χ^2, where χ^2 is given by[30]

$$\chi^2=(1/n)\sum_i[Y(\theta_i)-W(\theta_i)]^2/E^2(\theta_i), \quad (14)$$

where $E(\theta_i)$ is the uncertainty assigned to the gamma-ray yield $Y(\theta_i)$ at angle θ_i, and n is the number of degrees of freedom.[31] A plot of χ^2 versus x will then show dips corresponding to possible solutions for at least one set of the allowed spins a and b. For a given value of χ^2 the probability that the set of a,b, and x used is the correct one can be found by referring to χ^2-probability tables.[30]

[30] G. J. Nijgh, A. H. Wapstra, and R. van Lieshout, *Nuclear Spectroscopy Tables* (North-Holland Publishing Company, Amsterdam, 1959).

[31] In the present application, $n=$ (number of angles at which data have been taken) -2. The expectation value of χ^2 defined by Eq. (14) is unity.

TABLE V. Angular distribution coefficients, $F_k(LL'ba)$ for various integer values of a and b.

		k									
		2			4			6			8
a	b	LL	$L, L+1$	$L+1, L+1$	LL	$L, L+1$	$L+1, L+1$	LL	$L, L+1$	$L+1, L+1$	$L+1, L+1$
1	0	0.7071	0.0000	0.0000							
	1	−0.3536	−1.0607	−0.3536							
	2	0.0707	0.4743	0.3536							
	3	−0.1010	0.3780	0.5303							
	4	−0.1768	0.3062	0.6010							
2	0	−0.5976	0.0000	0.0000	−1.0690	0.0000	0.0000				
	1	0.4183	−0.9354	−0.2988	0.0000	0.0000	0.7127				
	2	−0.4183	−0.6124	0.1281	0.0000	0.0000	−0.3054				
	3	0.1195	0.6547	0.3415	0.0000	0.0000	0.0764				
	4	−0.1707	0.5051	0.4482	−0.0085	−0.0627	−0.0297				
	5	−0.2988	0.4009	0.4618	0.0040	−0.0815	−0.1093				
3	0	−0.8660	0.0000	0.0000	0.2132	0.0000	0.0000	1.3056	0.0000	0.0000	
	1	−0.4949	−0.4629	−0.6495	−0.4467	1.0446	0.0355	0.0000	0.0000	−0.9792	
	2	0.3464	−0.9487	−0.1237	0.0000	0.0000	0.6701	0.0000	0.0000	0.0000	
	3	−0.4330	−0.4330	0.2268	0.0000	0.0000	−0.4467	0.0000	0.0000	0.0000	
	4	0.1443	0.7217	0.3093	0.0000	0.0000	0.1489	0.0000	0.0000	0.0000	
	5	−0.2062	0.5455	0.3608	−0.0203	−0.1343	−0.0549	0.0000	0.0000	−0.0099	
	6	−0.3608	0.4270	0.3346	0.0097	−0.1720	−0.1946	0.0008	0.0063	−0.0014	
4	1	−0.7835	−0.2714	−0.8234	0.1453	0.7549	0.3017	0.4214	−1.0218	−0.0034	1.1847
	2	−0.4477	−0.5297	−0.4701	−0.3044	0.9004	−0.0484	0.0000	0.0000	−0.7585	0.0000
	3	0.3134	−0.9402	−0.0448	0.0000	0.0000	0.6088	0.0000	0.0000	0.0000	0.0000
	4	−0.4387	−0.3354	0.2646	0.0000	0.0000	−0.4981	0.0000	0.0000	0.0000	0.0000
	5	0.1595	0.7568	0.2849	0.0000	0.0000	0.1937	0.0000	0.0000	0.0000	0.0000
	6	−0.2279	0.5641	0.2991	−0.0298	−0.1844	−0.0687	0.0000	0.0000	−0.0265	0.0000
5	2	−0.7360	−0.3291	−0.6825	0.1159	0.7774	0.0802	0.2420	−0.7574	−0.0290	0.7785
	3	−0.4206	−0.5563	−0.3680	−0.2428	0.8030	−0.0773	0.0000	0.0000	−0.6049	0.0000
	4	0.2944	−0.9309	0.0000	0.0000	0.0000	0.5666	0.0000	0.0000	0.0000	0.0000
	5	−0.4416	−0.2739	0.2831	0.0000	0.0000	−0.5230	0.0000	0.0000	0.0000	0.0000
	6	0.1698	0.7783	0.2669	0.0000	0.0000	0.2241	0.0000	0.0000	0.0000	0.0000
6	3	−0.7051	−0.3575	−0.5915	0.0997	0.7581	−0.0296	0.1708	−0.6062	−0.0342	0.5502
	4	−0.4029	−0.5698	−0.3022	−0.2088	0.7383	−0.0902	0.0000	0.0000	−0.5124	0.0000
	5	0.2820	−0.9232	0.0288	0.0000	0.0000	0.5370	0.0000	0.0000	0.0000	0.0000
	6	−0.4432	−0.2315	0.2935	0.0000	0.0000	−0.5370	0.0000	0.0000	0.0000	0.0000

The least-squares fits were performed using the Oxford University Mercury computer. Since $-\infty \leq x \leq \infty$, some nonlinear scale is convenient. The variable used was arctan x which was varied in 5° steps from −90° to +90°. The program used could treat up to three gamma-ray transitions originating, either directly or in subsequent cascades, from the level with spin a with all but one of the mixing parameters fixed and the remaining one variable. In order to use the linear least-squares fitting procedure with two or more gamma transitions it is necessary to normalize the total intensities of the transitions to the same value. This was done by making a least-squares fit of each measured distribution to the Legendre polynomial expansion $I(\gamma)[1+a_2P_2(\cos\theta)+a_4P_4(\cos\theta)]$ and dividing the $Y(\theta_i)$ for a given transition by the $I(\gamma)$ obtained for that transition. The $I(\gamma)$ generated by these fits were also used in obtaining the branching ratios for the various observed modes of decay.

The particle counter used in this work was not an ideal counter placed at 180° with respect to the beam, but was a small annulus with its center at 180° and its inner and outer edges subtending angles at the target center of 172° and 168°, respectively. The effect of this on the populations of the magnetic substates in the present case is to allow substates with $|\alpha|>1$ to be populated to a small extent. Litherland and Ferguson[17] have considered this problem in general. Using their results we find that for our experimental conditions it is very unlikely that $P(2)>0.03$ and that the population of substates with $|\alpha|>2$ is negligible. We shall refer to the small but non-negligible population of the $\alpha=\pm 2$ substates as the finite size effect. To estimate this effect the arctan x versus χ^2 fitting was done twice for a >1, once with $P(2)=0$ and once assuming $P(2)=0.1P(1)$. This latter relation was chosen since it gave values of $P(2)$ in the range 0.03 to 0.05 near the interesting values of arctan x for all the cases considered.

C. Lifetime Limits

In the course of this work it was found that all of the first ten excited states of F^{18} except the 1.125-MeV level have mean lifetimes less than 10^{-8} sec. This limit was

TABLE VI. Angular distribution coefficients, $F_k(LL'ba)$ for various half-integer values of a and b.

		k									
		2			4			6			8
a	b	LL	$L,L+1$	$L+1, L+1$	LL	$L,L+1$	$L+1, L+1$	LL	$L,L+1$	$L+1, L+1$	$L+1, L+1$
3/2	1/2	0.5000	−0.8660	−0.5000							
	3/2	−0.4000	−0.7746	0.0000							
	5/2	0.1000	0.5916	0.3571							
	7/2	−0.1429	0.4629	0.5000							
	9/2	−0.2500	0.3708	0.5409							
5/2	1/2	−0.5345	−0.3780	−0.8018	−0.6172	1.0911	0.1543				
	3/2	0.3742	−0.9487	−0.1909	0.0000	0.0000	0.7054				
	5/2	−0.4276	−0.5071	0.1909	0.0000	0.0000	−0.3968				
	7/2	0.1336	0.6944	0.3245	0.0000	0.0000	0.1176				
	9/2	−0.1909	0.5297	0.4009	−0.0147	−0.1019	−0.0444				
	11/2	−0.3341	0.4173	0.3924	0.0070	−0.1314	−0.1602				
7/2	1/2	−0.8183	−0.2113	−0.9274	0.1709	0.6621	0.5128	0.6528	−1.1798	0.0435	
	3/2	−0.4676	−0.5051	−0.5455	−0.3582	0.9671	−0.0190	0.0000	0.0000	−0.8704	
	5/2	0.3273	−0.9449	−0.0779	0.0000	0.0000	0.6367	0.0000	0.0000	0.0000	
	7/2	−0.4364	−0.3780	0.2494	0.0000	0.0000	−0.4775	0.0000	0.0000	0.0000	
	9/2	0.1528	0.7416	0.2962	0.0000	0.0000	0.1737	0.0000	0.0000	0.0000	
	11/2	−0.2182	0.5563	0.3273	−0.0253	−0.1614	−0.0627	0.0000	0.0000	−0.0183	
9/2	3/2	−0.7569	−0.3062	−0.7444	0.1281	0.7774	0.1693	0.3077	−0.8714	−0.0213	0.9633
	5/2	−0.4325	−0.5455	−0.4129	−0.2684	0.8465	−0.0660	0.0000	0.0000	−0.6714	0.0000
	7/2	0.3028	−0.9354	−0.0197	0.0000	0.0000	0.5857	0.0000	0.0000	0.0000	0.0000
	9/2	−0.4404	−0.3015	0.2752	0.0000	0.0000	−0.5125	0.0000	0.0000	0.0000	0.0000
	11/2	0.1651	0.7687	0.2752	0.0000	0.0000	0.2102	0.0000	0.0000	0.0000	0.0000
11/2	5/2	−0.7191	−0.3454	−0.6326	0.1067	0.7692	0.0171	0.1998	−0.6718	−0.0326	0.6460
	7/2	−0.4109	−0.5641	−0.3319	−0.2237	0.7676	−0.0849	0.0000	0.0000	−0.5532	0.0000
	9/2	0.2876	−0.9269	0.0158	0.0000	0.0000	0.5505	0.0000	0.0000	0.0000	0.0000
	11/2	−0.4425	−0.2509	0.2890	0.0000	0.0000	−0.5309	0.0000	0.0000	0.0000	0.0000

set from a simple consideration of the linear distribution of gamma-ray emission along a beam of recoiling nuclei. The evidence for this limit is discussed in Sec. IVC.

This lifetime limit imposes an upper limit on the multipolarities of the observed transitions and therefore on the spins of the emitting levels. For a given level these limits will depend on the branching ratios and energies of the various transitions so that it is not practical to give one over-all limit. Instead, it is convenient to convert the lifetime limit for a given decay mode into a limit on the transition strength in Weisskopf units where, for a given multipolarity, the Weisskopf unit is the Weisskopf estimate[32] for the radiative width $\Gamma_{\gamma W}$ in eV evaluated using a nuclear radius constant of 1.2 F. The lifetime limit $\tau<10^{-8}$ sec corresponds to a lower limit on the transition strength for a given multipolarity of 6.58×10^{-8} (B.R./100) $\times\Gamma_{\gamma W}{}^{-1}$ Weisskopf units, where B.R. is the branching ratio for the transition expressed in percent. For a transition with two competing multipolarities, L and $L+1$, the lower limit on the transition strength is obtained by multiplying the above expression by $1/(1+x^2)$ and $x^2/(1+x^2)$, respectively, where x is the mixing parameter of the transition.

[32] D. H. Wilkinson, in *Nuclear Spectroscopy*, Part B, edited by F. Ajzenberg-Selove (Academic Press Inc., New York, 1960), p. 862 ff.

The general survey of the measured transition strengths in light nuclei and the various theoretical sum rule limits for electric transitions given by Wilkinson[32] gives us some guide to the maximum transition strengths which are reasonably possible. From these two sources we conclude that an upper limit to electric transitions in F^{18} of 100 Weisskopf units seems reasonably safe. For magnetic transitions we also take 100 Weisskopf units as an upper limit unless the transition has $\Delta T=0$. In this case the transition will be inhibited[33] by a factor which is, on the average, ~100, and we take 10 Weisskopf units as an upper limit and consider a strength of about 1 Weisskopf unit as unlikely.

Lifetime measurements have previously been made[9,10] for some of the levels studied in the present work. The implications of these measurements will be discussed. However, the assignment of spins from this study is made as independently as possible of these previous experimental results.

IV. EXPERIMENTAL RESULTS

A. The 1.70-MeV Level

The (p,γ) correlations for this level in F^{18} supply a good illustration of the method of analysis and so will be considered first. This state decays by gamma emis-

[33] E. K. Warburton, Phys. Rev. Letters **1**, 68 (1958).

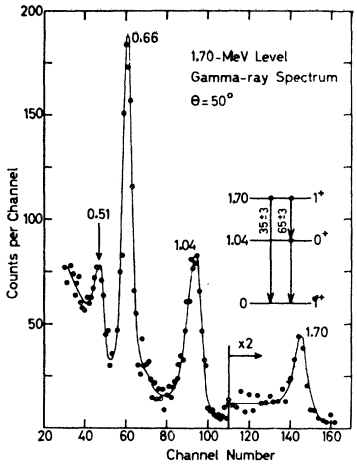

FIG. 4. Spectrum of gamma rays observed at 50° to the beam in coincidence with the proton group populating the F^{18} 1.70-MeV level in the $O^{16}(He^3,p)F^{18}$ reaction at a He^3 energy of 3.60 MeV. Except for the 0.51-MeV annihilation radiation, the gamma-ray peaks correspond to the transitions indicated in the decay scheme. The randoms have been subtracted.

sion to the ground state and 1.04-MeV state of F^{18}. The decay thus involves the only three bound states in this nucleus with well established spin-parity assignments. It was studied in order to find the $E2/M1$ mixing ratio for the decay to the ground state. At the same time it will be seen that a natural outcome of this study is a further independent confirmation of the $J^\pi=1^+$ assignment to this state at 1.70 MeV in F^{18}.[34]

The measurements were made at an incident He^3 energy of 3.60 MeV in the first series of measurements. Coincidence gamma-ray spectra were recorded at 20°, 35°, 50°, 65°, and 90° to the beam axis. The 50° gamma-ray spectrum with the random spectrum subtracted is shown in Fig. 4. The 0.51-MeV gamma ray, which is present in all the coincidence spectra, arises partly from real coincidences following pair production in material in the vicinity of the NaI crystal and partly from real coincidences with the background underlying the proton peak in the annular detector (see Fig. 2). The other three gamma-rays which are identified in Fig. 4 arise from the decay of the 1.70-MeV level to the F^{18} ground state and 1.04-MeV level. As for all the F^{18} levels studied, angular distributions were obtained for each gamma ray by summing a given pulse-height region for each of the spectra and subtracting the contributions of higher energy gamma rays. For instance, in the present case the $1.70\rightarrow 0$ distribution was obtained from the sum of counts between channels 106 and 160 with randoms subtracted while the $1.04\rightarrow 0$ distribution was obtained from the sum of counts between channels 80 and 104 with the contribution to this pulse-height region of randoms and the 1.70-MeV gamma ray subtracted. The subtraction of the contributions of higher energy gamma rays was facilitated by monoenergetic spectral shapes obtained from radioactive sources and from coincidence spectra for simple decay modes recorded in this investigation and in work[20] on S^{32} and Ca^{40}.

The angular distributions of the three gamma rays observed in the decay of the 1.70-MeV level are shown in Fig. 5. The distributions are plotted as a function of $\cos^2\theta$ in order to illustrate that there is no evidence for terms in $P_k(\cos\theta)$ with $k>2$. The distributions shown in Fig. 5 were fitted by the least-squares method to $W(\theta)=I(\gamma)[1+a_2P_2(\cos\theta)]$ with results for a_2 of -0.37 ± 0.06, -0.56 ± 0.04, and 0.01 ± 0.05 for the $1.70\rightarrow 0$, $1.70\rightarrow 1.04$, and $1.04\rightarrow 0$ transitions, respectively. The values of $I(\gamma)$ from the least-squares fits were used, together with tables of efficiences and photofractions for gamma rays detected in NaI(Tl) crystals,[35] to obtain the branching ratios of the 1.70-MeV level. The measured branching ratios were $(35\pm3)\%$ and $(65\pm3)\%$ for the $1.70\rightarrow 0$ and $1.70\rightarrow 1.04$ transitions, respectively, in fair agreement with the earlier results of Kuehner, Almqvist, and Bromley[11] which were 31% and 69%, respectively.

The angular distributions for the $1.70\rightarrow 0$ and $1.70\rightarrow 1.04$ transitions were fitted simultaneously as a function of the $(L+1)/L$ amplitude ratio x for the $1.70\rightarrow 0$ transition. This was done using the computer program appropriate for two distributions with one

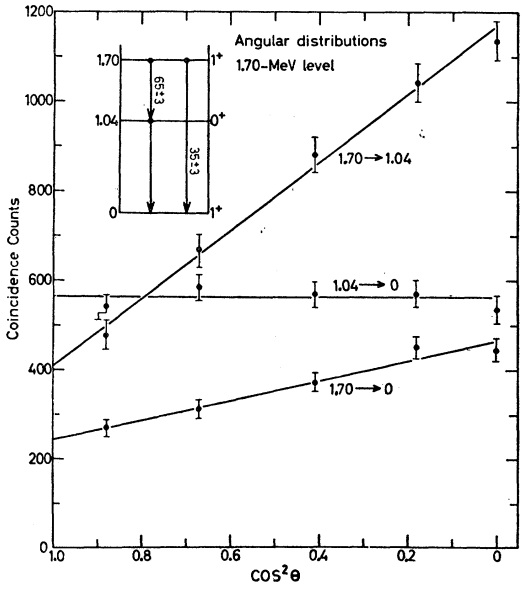

FIG. 5. Angular distributions measured at a He^3 energy of 3.60 MeV for the three gamma rays arising from the decay of the F^{18} 1.70-MeV level.

[34] In the remainder of this paper the usual symbol J will be used to denote the total angular momentum (spin) of a nuclear state. The symbols a, b, c, etc., were used in the theoretical formulas given in the last section because that was the notation used by the originators of the method used in this work (Ref. 17).

[35] S. H. Vegors, L. L. Marsden, and R. L. Heath, Phillips Petroleum Company, Atomic Energy Division (unpublished), IDO-16370.

variable mixing ratio (see Sec. IIIB) and assuming $J=1$ and 0 for the F^{18} ground state and 1.04-MeV level. The results are shown in Fig. 6 which gives χ^2 versus arctan x curves for spin assignments of 1, 2 and 3 to the 1.70-MeV level. Spin assignments greater than 3 are not considered since such assignments would lead to lifetimes for the $1.70 \rightarrow 1.04$ transition longer than 10^{-8} sec (see Sec. IIIC). Figure 6 illustrates clearly that the measured distributions are inconsistent with $J=2$, and 3, but allow an assignment of $J=1$. Thus the present results are consistent with the spin sequence 1, 0, 1 for the F^{18} levels at 0, 1.04, and 1.70 MeV, in agreement with previous results, and demand $J=1$ for the 1.70-MeV level assuming $J=1$ and 0 for the F^{18} g.s. and 1.04-MeV level.

From Fig. 6 we see that two values of the $E2/M1$ mixing ratio are allowed. These are $x=0.49\pm0.06$ and $x=2.05\pm0.3$.

We now wish to consider the possible effects of the finite size of the proton counter (finite size effects). The reason for the very large values of χ^2 shown in Fig. 6 for the $J=2$ and $J=3$ curves can be seen by inspection of the theoretical angular distributions. For population of the $\alpha=0$ and ±1 substates only, both $2 \rightarrow 0$ and $3 \rightarrow 0$ transitions must have positive values of a_2 while for a $3 \rightarrow 0$ transition a_4 must be positive also. Both restrictions are clearly inconsistent with the experimental results for the $1.70 \rightarrow 1.04$ transition. In order to bring the theoretical distributions for $J=2$ and 3 into agreement with the experimental distributions we find that for $J=2$ the 1.70-MeV level would need to be formed predominantly in its $\alpha=\pm2$ substates and for $J=3$ predominantly in its $\alpha=\pm3$ substates. These restrictions are obviously inconsistent with the geometrical arragement used. For $J=1$ there is no question of formation in substates other than $\alpha=0$ and ±1. Thus the conclusions drawn from Fig. 6 cannot be altered by any conceivable effects due to the finite size of the proton counter.

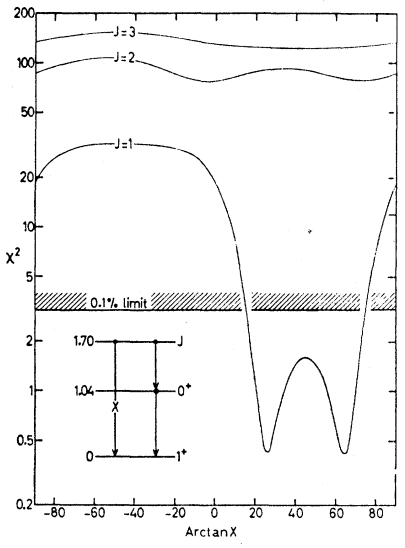

FIG. 6. χ^2 versus arctan x for the decay of the F^{18} 1.70-MeV level at $E_{He^3}=3.60$ MeV. The $1.70 \rightarrow 1.04$ and $1.70 \rightarrow 0$ angular distributions are fitted simultaneously as a function of the $(L+1)/L$ amplitude ratio, x, for the $1.70 \rightarrow 0$ transition. For a correct solution, the expectation value of χ^2 is unity and the probability of χ^2 exceeding the value of χ^2 marked as the 0.1% limit is 0.1%. Curves are shown assuming $J=1$, 2, and 3 for the spin of the 1.70-MeV level.

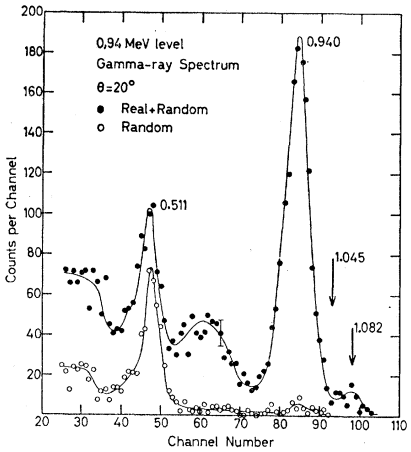

FIG. 7. Spectrum of gamma rays observed at 20° to the beam in coincidence with the proton group populating the F^{18} 0.940-MeV level in the $O^{16}(He^3,p)F^{18}$ reaction at a He^3 energy of 3.75 MeV. The spectrum of reals plus randoms is given by the closed circles. The randoms spectrum is given by the open circles.

The lifetime of the 1.70-MeV level has been measured to be $(2\pm1)\times10^{-12}$sec.[10] Combining this value with our measurement of the $1.70 \rightarrow 0$ branching ratio and the value $x=0.49\pm0.06$ for the mixing ratio of the $1.70 \rightarrow 0$ transition gives 15 ± 8 Weisskopf units for the $M2$ $1.70 \rightarrow 0$ transition strength if the 1.70-MeV level were $J^\pi=1^-$. Since this value is improbably large for a $\Delta T=0$ transition we have additional confirmation that the 1.70-MeV level has even parity.

B. The 0.940-MeV Level

The angular distribution of the ground-state transition from the first excited state of F^{18} at 0.940 MeV was measured first at a bombarding He^3 energy of 3.75 MeV. This energy was chosen after an excitation function had shown that the yield of the p_1 group relative to the nearby unresolved triplet $p_{2,3,4}$ had a local maximum at $E_{He^3}=3.75$ MeV (Fig. 2). The contribution to the gamma-ray spectra of de-excitation gamma rays from the F^{18} 1.043-, 1.082-, and 1.125-MeV levels (corresponding to p_2, p_3, and p_4) was minimized further by setting a narrow gate on the p_1 peak. This would have excluded any contribution from the 1.125-MeV level and suppressed contributions from the 1.082- and 1.045-MeV levels. The exclusion of contributions from the 1.125-MeV level is important since this level decays by cascade through the 0.940-MeV level.

Gamma-ray spectra were recorded at 20, 35, 42.5, 50, 65, and 90°. The 20° spectrum is shown in Fig. 7.

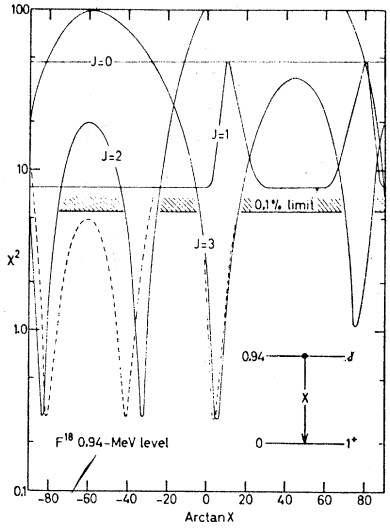

FIG. 8. χ^2 versus arctan x for the F^{18} $0.94 \rightarrow 0$ transition and assumed spins of 0, 1, 2 and 3, for the 0.94-MeV level. The full curves are for population of the $\alpha=0, \pm 1$ magnetic substates only, while the broken curves are for $P(2)=0.1P(1)$.

This spectrum is shown without the randoms subtracted. The randoms spectrum is also shown to illustrate the relative contribution of randoms in a typical case. It is seen that most of the random counts are due to annihilation radiation. From Figs. 2 and 7 it appears that the yield of 1.08-MeV gamma rays is appreciably larger than that of 1.04-MeV gamma rays. In any case the small contribution of these two gamma rays was easily subtracted to give the angular distribution of the 0.940-MeV gamma ray. A least-squares Legendre polynomial fit to this distribution gave $a_2=+(0.32\pm0.06)$, $a_4=-(0.05\pm0.07)$.

The angular distribution of the 0.940-MeV transition to the 1^+ F^{18} ground state was fitted by the χ^2 computer program for a single gamma ray with a variable mixing parameter x, assuming $J=2$ or 3 for the 0.940-MeV level. Spin assignments of 4 and greater were excluded by the lifetime limit[9] $\tau<2\times10^{-10}$ sec (this limit corresponds to $E3$ and $M3$ strengths of 6.8×10^5 and 1.58×10^7 Weisskopf units, respectively), while $J=0$ and 1 were excluded by former (p,γ) measurements[11,36] which gave conclusive evidence for nonzero values of a_2 and a_4. The χ^2 fit allowed both $J=2$ and 3 with two solutions for x with $J=2$ and one solution with $J=3$. The solution for $J=3$ gave $P(1)=0.50$, $P(0)=0$ which, if the spin is actually $J=3$, is the worst formation condition for exclusion of $J=2$. Thus the angular distribution was repeated at a different incident energy, $E_{He^3}=3.0$ MeV. This was done during the second series of measurements so that the NaI(Tl) crystal could be rotated between 0° and 90°. In this case there was no discernible population of the F^{18} 1.082- and 1.125-MeV states or evidence of gamma rays from them but the contribution of the 1.045-MeV gamma ray to the total gamma-ray yield amounted to 30%. However, the subtraction of this isotropic contribution was straightforward. The angular distribution obtained at 3.0 MeV is characterized by $a_2=+(0.36\pm0.04)$, $a_4=-(0.22\pm0.05)$. The χ^2 fits for $J=0$, 1, 2 and 3 are shown by the solid curves plotted in Fig. 8. It is apparent from Fig. 8 that this angular distribution excludes $J=0$ and 1 in agreement with previous (p,γ) work, but still allows solutions for both $J=2$ and $J=3$. In this case also, the analysis indicated that the 0.94-MeV level was formed predominantly in its $\alpha=\pm1$ substates for $J=3$. The rather strange behavior of the χ^2 curve for $J=1$ occurs because there are two roots for the angular distribution function, $F_2(11)$. These are $x=0.17$ and 5.80 (arctan $x=10°$ and 80°) and at these values of x the angular distribution of a transition between two $J=1$ states must be isotropic so that χ^2 for $J=1$ equals χ^2 for $J=0$ at these roots. The solution for $J=3$ at arctan $x=75°$ ($x=3.43$) shown in Fig. 8 is shown to be most improbable by the angular distribution measured at $E_{He^3}=3.75$ MeV. In that case the minimum in χ^2 lay slightly above the 2% probability limit. In any case this solution can be excluded since it corresponds to almost pure octupole radiation, i.e., $x^2>13$ and is therefore incompatible with the lifetime limit.

The dashed curves for $J=2$ and 3 in Fig. 8 give the χ^2 curves with $P(2)=0.1P(1)$ and thus give our estimate of finite size effects (see Sec. IIIB). It is seen that this effect is rather important for $J=2$ but less so for $J=3$.

To summarize the results of this measurement, we find that the 0.940-MeV level is $J=3$ with an octupole-quadrupole mixing ratio of $x=+(0.08\pm0.08)$ or $J=2$ with a quadrupole-dipole mixing parameter $x=-(0.60\pm0.05)$ or $-(9.5_{-2.4}^{+4.8})$. For both $J=2$ and 3, the solutions for x are averages from both measurements and include our estimate of the finite size effect. For $J=2$ the uncertainties associated with x are considerably less than for either of the individual measurements. The reason for this is that the values obtained for x at $E_{He^3}=3.0$ and 3.75 MeV were in rather poor agreement and the region of overlap was small.

The lifetime limit $\tau<2\times10^{-10}$ sec for the $\Delta T=0$, $0.94\rightarrow0$ transition corresponds to lower limits on the strength of this transition of 1.9 and 43.5 Weisskopf units for $E2$ and $M2$ radiation, respectively. Thus, we assign even parity to the 0.94-MeV level if $J=3$. If $J=2$, then the lower limits on the $M2$ strength are 13 and 43 Weisskopf units for $x=-(0.60\pm0.05)$ and $-(9.5_{-2.4}^{+4.8})$, respectively, and we assign even parity if $J=2$ also.

We now show that the present results combined with the linear polarization results of Litherland and Gove[37]

[36] S. Hinds and B. M. Hinds, Nucl. Phys. 48, 690 (1963).

[37] A. E. Litherland and H. E. Gove, Bull. Am. Phys. Soc. 3, 200 (1958).

eliminate the possibility $J=2$ for the 0.94-MeV level. For the linear polarization measurement, Litherland and Gove used the $O^{16}(He^3,p)F^{18}$ reaction and measured the linear polarization of the $0.94\rightarrow 0$ transition at 90° to the beam. They found $P=2.5\pm0.3$, where P is the ratio of the linear polarization intensity parallel to the plane defined by the reaction to the linear polarization intensity perpendicular to the plane of the reaction. The angular distribution relative to the beam (protons unobserved) of the 0.94-MeV transition was characterized by $a_2=+0.25$, $a_4=0.0$.[38] In terms of the quantities defined in Sec. IIIA, the quantity P is given theoretically for a dipole-quadrupole mixture by[39]

$$P=\left[\frac{1+a_2+a_4+[4x/(1+x^2)]\rho_2(a)F_2(12ba)}{1-2a_2-\frac{1}{4}a_4-[4x/(1+x^2)]\rho_2(a)F_2(12ba)}\right]^{1-2\sigma}, \quad (15)$$

where, as before, σ is 0 for a $M1,E2$ mixture and 1 for an $E1,M2$ mixture. It is apparent that for pure dipole or pure quadrupole radiations, i.e., $[x/(1+x^2)]=0$, the predicted value of P for $a_2=+0.25$, $a_4=0$ is 2.5 for $\sigma=0$, and 0.4 for $\sigma=1$. Thus the linear polarization measurement is consistent with a $J^\pi=3^+$ assignment for the 0.94-MeV level and can be shown to definitely exclude a $J^\pi=3^-$ assignment if $x=-(0.08\pm0.08)$. For a $J=2$ assignment to the 0.940-MeV level and $a_2=0.25$, $a_4=0$, Eq. (15) can be written as

$$P=\left[\frac{2.5-f(x)}{1+f(x)}\right]^{1-2\sigma}, \quad (16)$$

where

$$f(x)=(2\sqrt{5})x/[1+(2\sqrt{5})x-0.7142x^2] \quad (17)$$

has been evaluated from Eq. (15) using Eq. (1) and Tables II and V. In Fig. 9 is shown a plot of P versus x for $M1,E2$ and $E1,M2$ mixtures. The measured value of P, 2.5 ± 0.3, is indicated as well as the two possible solutions for x obtained in the present experiment. It is clear that the solution $x=-(0.60\pm0.05)$ is consistent with the polarization measurement if the 0.940-MeV level has odd parity but not if it has even parity. Since we have used the lifetime limit to rule against an $E1,M2$ mixture we can exclude the solution $x=-(0.60\pm0.05)$.

The solution $x=-(9.5_{-2.4}{}^{+4.8})$ is in disagreement with the polarization measurement for either parity assignment. The disagreement is quite marked for odd parity so that we can exclude the possibility of an $E1,M2$ mixture with $x=-9.5_{-2.4}{}^{+4.8}$ from the linear polarization results as well as from the lifetime limit. For a $M1,E2$ mixture, however, the degree of disagreement is not readily apparent from Fig. 9 but can be shown to rule against the solution $x=-9.5_{-2.4}{}^{+4.8}$ with a sufficiently high probability to allow us to safely exclude the possibility that the 0.940-MeV level has $J=2$. To show this we first must calculate the uncertainty in the theoretical expression for P [Eqs. (15) or (16)] due to the experimental uncertainties in the measurements[37,38] of a_2 and a_4.[40] After doing this we find that the linear polarization measurement demands arctan $x=(90\pm1)°$ or $(0\pm2)°$ if the 0.940-MeV level is $J^\pi=2^+$; while our (p,γ) results give the solution arctan $x=(84\pm2)°$. The probability of overlap between the two measurements was calculated for the two solutions arctan $x=(90\pm1)°$ and $(84\pm2)°$ using the results shown in Fig. 8 for the (p,γ) measurement and the calculation which included the uncertainties in a_2 and a_4 for the linear polarization measurement. The result is that the probability of overlap is $\leq1.3\%$ so that the solution arctan $x=(84\pm2)°$ can be excluded with a probability of 98.7%.[41]

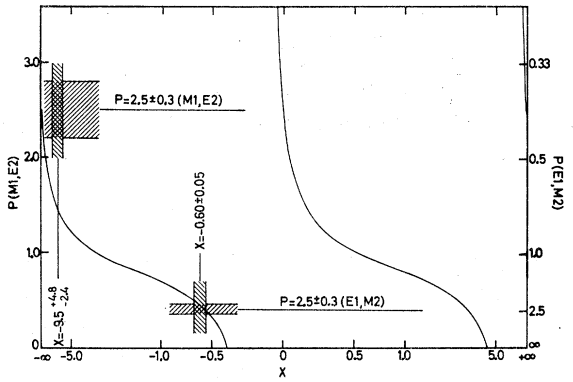

FIG. 9. The curve shows the linear polarization ratio P (see text) as a function of the dipole-quadrupole mixing parameter x for a gamma-ray transition between a $J=2$ initial state and a $J=1$ final state. The left-hand scale should be used for a $M1,E2$ mixture (no parity change) and the right-hand scale for an $E1,M2$ mixture (parity change). The experimental value of P obtained for the F^{18} $0.94\rightarrow0$ transition by Litherland and Gove is indicated for both $M1,E2$ and $E1,M2$ mixtures. The values of x allowed by the present (p,γ) results are shown and the overlap between the theoretical curve for P, the experimental measurement of P, and these values of x is indicated.

We find, then, that the lifetime limit of Lowe and McClelland,[9] the linear polarization measurement of Litherland and Gove,[37] and the present (p,γ) measurements, taken together, demand $J^\pi=3^+$ for the 0.940-MeV level.

The $0.940\rightarrow0$ transition is then an $E2,M3$ mixture. For an upper limit to the $M3$ strength of 10 Weisskopf units the lifetime limit $\tau<2\times10^{-10}$ sec gives the limit $|x|<2.5\times10^{-4}$ so that we expect x to differ negligibly from zero. For both angular distribution measurements on the $0.94\rightarrow0$ transition the probability that the

[38] Private communication from A. E. Litherland. These numbers do not appear in Ref. 37. We would like to thank Dr. Litherland for making them available to us.

[39] L. W. Fagg and S. S. Hanna, Rev. Mod. Phys. **31**, 711 (1959).

[40] The uncertainties associated with a_2 and a_4 were not available to us. We assumed uncertainties of ±0.05 for both coefficients. These seem to us to be conservative estimates for the type of measurement involved.

[41] We note that the finite size effect on the χ^2 minimum for $J=2$ (see Fig. 8) is such as to decrease the overlap between the (p,γ) and linear polarization results. Thus we have no worries on this score.

transition is pure quadrupole was less than 10% assuming no finite size effect and ~40% with our estimate of the finite size effect. This is the clearest evidence obtained in this work for the population of the $\alpha=\pm 2$ magnetic substates due to the finite size of the proton counter.

C. The 1.082-MeV Level

The study of the (p,γ) angular correlation for the third excited state of F^{18} at 1.082 MeV was complicated by the fact that neither the proton groups p_2, p_3, and p_4 corresponding to the F^{18} 1.045-, 1.082-, and 1.125-MeV levels, nor the gamma rays from the 1.045- and 1.082-MeV levels were resolved. The 1.045- and 1.082-MeV levels decay to the F^{18} ground state, while the 1.125-MeV level decays to the 0.940-MeV level. Thus the gamma radiation from the triplet $p_{2,3,4}$ consists of four gamma rays with energies of 0.185, 0.940, 1.045, and 1.082 MeV.

During the course of the study of the 1.082-MeV level, it was found that the 0.185- and 0.940-MeV gamma rays emitted from the 1.125-MeV level had angular distributions which could be approximately described by a $1/r^2$ variation, r being the distance from the front face of the NaI(Tl) crystal to the beam stop. Since this distance varied from 28 to 12.7 cm as the 12.7×15.2 cm crystal swung from 90° to 0° with respect to the beam, these angular distributions were strongly peaked at 0°. The explanation for this behavior is that since the protons were detected at 180°, the resulting F^{18*} nuclei recoiled at 0°. Escaping from the thin target they then came to rest in the beam stop before decaying. This is expected since the lifetime of the F^{18} 1.125-MeV level is $(1.9\pm 0.5)\times 10^{-7}$ sec.[12] For the energies involved, the F^{18*} recoils travelled about 80 cm in this time. We note that this behavior was not observed for any other of the first ten excited states of F^{18}, and an upper limit of 10^{-8} sec can be placed on the lifetimes of these states from a more detailed consideration of the amount of forward peaking consistent with the observed angular distributions. This is a sharper limit than that which could be placed by the mere fact of observation of (p,γ) coincidences with the 1×10^{-7} or 2×10^{-7} sec resolving time used in this work.

Evidence is presented in Sec. IIID to show that the F^{18} 2.10-MeV level has a $(34\pm 4)\%$ branch to the 1.08-MeV level. The establishment of this decay mode and the lifetime limit, $\tau<10^{-8}$ sec, for the 1.08-MeV level can be used in conjunction with previous work to sharpen appreciably the lifetime limit for this level. Lowe and McClelland[9] set a lifetime limit, $\tau<2\times 10^{-10}$ sec, for the F^{18} 0.940-MeV level from observations of the time spectrum of the $0.940\rightarrow 0$ transition. They used a pulsed Van de Graaff beam, a thick SiO_2 target, and the $O^{16}(He^3,p)O^{16}$ reaction. Because of the proximity in energy, the coincidence gate set on the 0.94-MeV gamma rays in their work would have been equally efficient for any 1.08-MeV gamma rays which were present. Thus their time spectrum can be used, in principle, to give a lifetime limit for the 1.08-MeV gamma ray as well. However, before this can be done, it is necessary to have a lifetime limit of about $\tau<10^{-8}$ sec or better for this level and to have an approximate number or limit for the fraction of counts due to the $1.08\rightarrow 0$ transition which are in the coincidence window. The lifetime limit is necessary to insure that the 1.08-MeV gamma rays arrive at the detector while the time spectrum is being recorded and are not lost in the background, while a knowledge of the fraction of 1.08-MeV gamma rays in the coincidence window is necessary to estimate the effect on the time spectrum for different assumed lifetimes for the 1.08-MeV state. The lifetime limit, $\tau<10^{-8}$ sec, obtained from the present results has been discussed above. An estimate of the fraction of 1.08-MeV gamma rays in the coincidence window can be obtained from the 90° excitation curves given by Kuehner *et al.*[11] for the 2.10-MeV level and other levels formed in the $O^{16}(He^3,p)F^{18}$ reaction and from the establishment of the $(34\pm 4)\%$ branch from the 2.10-MeV level to the 1.08-MeV level. (Kuehner *et al.*[11] do not give an excitation curve for the 1.08-MeV level itself.) Using these data J. Lowe[42] obtained a lower limit of 10% for the intensity of 1.08-MeV gamma rays in the window relative to the combined intensities of the 0.94-, 1.04-, and 1.08-MeV gamma rays. Using this limit he finds that the time spectrum obtained by Lowe and McClelland[9] can be interpreted to give a limit on the mean lifetime of the F^{18} 1.08-MeV state of $\tau<2\times 10^{-10}$ sec. This is the same limit Lowe and McClelland set for the 0.940-MeV level.

The main difficulty encountered in the (p,γ) angular distribution measurements on the $1.08\rightarrow 0$ transition was the problem of separating the contributions to the gamma-ray spectra of the 1.04- and 1.08-MeV gamma rays. To minimize the contribution of the 1.04-MeV gamma ray, a visual inspection of the proton spectra was made as the He^3 bombarding energy was varied in 10-keV steps in order to find energies at which the yield of p_3 was a maximum compared to that of p_2. Two local maxima were found at bombarding energies of 3.45 and 3.60 MeV. At both energies the average energy and width of the group $p_{2,3,4}$ was consistent with no feeding of the 1.045-MeV level and feeding of both the 1.082- and 1.125-MeV levels.

The composition of the proton group, $p_{2,3,4}$ was examined further by observations on the gamma rays in coincidence with it. At both bombarding energies gamma rays of 0.185 and 0.940 MeV from the decay of the 1.125-MeV level were observed as well as 1.08-MeV gamma rays. The gate set on the group $p_{2,3,4}$ excluded the protons (p_1) feeding the 0.940-MeV level and would have excluded about one-third of the protons (p_2)

[42] J. Lowe, (private communication).

feeding the 1.045-MeV level. There was no evidence for 1.045-MeV gamma rays at either bombarding energy.

Since the lifetime of the F^{18} 1.125-MeV level is approximately equal to the (p,γ) resolving time, the efficiency for detecting gamma rays from this level will be less than for the 1.082-MeV level. Correcting for this effect, the relative contributions of p_3 and p_4 in the unresolved $p_{3,4}$ proton group were estimated from the gamma-ray spectra. The intensity ratio of p_4 to p_3 was about unity at 3.45 MeV and 0.3 at 3.60 MeV. With this knowledge the expected shape and mean energy of the unresolved group $p_{3,4}$ could be synthesized and compared to experiment to yield upper limits on the relative contribution of p_2 to this group. In this manner it was found that the contribution of the 1.045-MeV gamma ray to the gamma-ray spectra was at most 20% of the 1.082-MeV gamma ray for the 3.45-MeV results and 30% for the 3.60-MeV results. To correct for the possible presence of this 1.045-MeV gamma ray, an isotropic contribution was subtracted from the two angular distributions measured for the 1.082-MeV gamma ray. This isotropic contribution was taken to be $(10\pm10)\%$ and $(15\pm15)\%$ of the 1.082-MeV gamma-ray intensity for the 3.45- and 3.60-MeV distributions, respectively.

The angular distributions obtained for the 1.082-MeV gamma ray were fitted to a Legendre polynomial expansion yielding $a_2=+(0.00\pm0.06)$, $a_4=+(0.04\pm0.08)$ at $E_{He^3}=3.45$ MeV and $a_2=+(0.01\pm0.08)$, $a_4=-(0.09\pm0.12)$ at $E_{He^3}=3.60$ MeV. Thus both distributions are isotropic within the errors of the measurement.

The χ^2 computer fit to the angular distribution of the 1.082-MeV gamma ray measured at a bombarding energy of 3.45 MeV is shown in Fig. 10 for assumed spins of $J=0$, 1, 2, and 3. Spin assignments of 4 or higher are ruled out by the lifetime limit $\tau<2\times10^{-10}$ sec. The results for the measurement at $E_{He^3}=3.60$ MeV are similar to those shown in Fig. 10. The dashed curves in Fig. 10 for $J=2$ and 3 are the χ^2 fits with $P(2)=0.1P(1)$ and thus give an estimate of the finite counter size effect. As the magnitude of the Legendre coefficients have previously indicated $J=0$ and 1 are quite consistent with the results, the latter for equal populations of the magnetic substates except near the two roots $x=0.17$ and 5.83 of $F_2(11)$ where the populations are not determined. For $J=2$ the two solutions for x are quite insensitive to the finite size effect and are at arctan $x=-(12\pm4)°$ and $+(81\pm3)°$ for $E_{He^3}=3.45$ MeV and $-(15\pm5)°$ and $+(85\pm4)°$ for $E_{He^3}=3.60$ MeV. We adopt the averages of the two measurements which are arctan $x=-(13\pm4)°$ and $+(83\pm4)°$, where the errors include our estimates of the finite size effect. It is seen that $J=3$ is not allowed if we neglect the finite size effect but that the χ^2 minimum near arctan $x=20°$ is quite sensitive to this effect. Thus $J=3$ with arctan $x\approx25°$ might be allowed if the magnitude of this effect was underestimated. However, we find that $J=3$ with arctan $x<10°$ $(x<0.176)$ gives χ^2 values near the 0.1% limit even if $P(2)$ is as large as 0.1, and a value of x as large as 0.176 for a quadrupole-octupole mixture can be ruled out by the lifetime limit $\tau<2\times10^{-10}$ sec since this limit combined with $x=0.176$ gives $E3$ and $M3$ speeds, respectively, of 8×10^3 and 1.8×10^5 times the Weisskopf estimate.

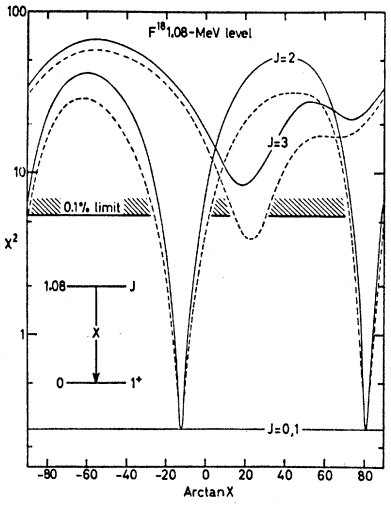

FIG. 10. χ^2 versus arctan x curves for the F^{18} 1.08 → 0 transition and assumed spins of $J=0$, 1, 2 and 3 for the 1.08-MeV level. The full curves are for population of the $\alpha=0, \pm1$ magnetic substates only, while the broken curves are for $P(2)=0.1P(1)$.

Kuehner *et al.*[11] measured the (p,γ) angular correlation for the 1.08-MeV level with the protons detected at 145° to the He^3 beam in the vertical plane and the 1.08-MeV gamma rays detected in the horizontal plane. They also measured the direct angular distribution (protons unobserved) of the sum of the 1.08- and 1.04-MeV gamma rays. In both cases they obtained isotropic distributions within the accuracy of the measurements. Their measurements and the present ones give rather strong evidence then that the 1.08 → 0 transition is isotropic (or nearly so) because of some property of the gamma-ray transition itself and not because of the formation mechanism. Thus it seems most probable that the 1.08-MeV level has either $J=0$ or is $J=1$ or 2 with a dipole-quadrupole mixture that insures isotropy for any directional distribution measurement. From the general properties of the triple correlation formulas[17] it can be seen that for $J=1$ the directional distribution of the 1.08 → 0 transition will be isotropic under any conditions (i.e., in the present case for any angles θ_p,ϕ_p of the proton counter) if $F_2(11)$ is zero, i.e., $x=0.17$ or 5.80,[43] a somewhat weaker statement can be made if $J=2$. We find in the present case that $x=-(0.23\pm0.07)$ or $8.1_{-2.5}^{+6}$ if $J=2$. The latter value is a solution which depends on cancellation of the a_4 coefficient due to a particular ratio of $P(0)/P(1)$. Thus this solution is unlikely since it

[43] This is seen easily from a theorem given by H. Van Rinsvelt and P. B. Smith, Physica **30**, 59 (1964).

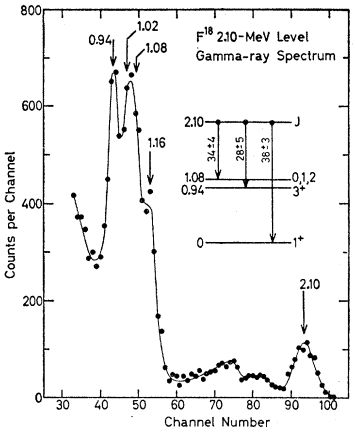

FIG. 11. Spectrum of gamma rays in coincidence with the proton group populating the F^{18} 2.10-MeV level in the $O^{16}(He^3,p)F^{18}$ reaction at an He^3 energy of 4.0 MeV. The spectrum is the sum of seven spectra taken at five different angles to the beam. The randoms have been subtracted. The positions of the gamma-ray peaks expected from the inserted decay scheme are indicated by the arrows.

would demand accidental cancellation in four separate measurements. For the solution $x=-(0.23\pm0.07)$, however, a_4 would be inherently small under any conditions since it is proportional to x^2, and assuming that a_4 is negligibly small, a_2 will be zero under any conditions if $x\simeq-0.213$ since this is one of the roots of $F_2(21)$.

We now consider the consequences of the lifetime limit, $\tau<2\times10^{-10}$ sec on the solutions for x for $J=1$ and 2. This limit corresponds to $E2$ and $M2$ strengths which are 0.96 and 21.5 times the Weisskopf estimate, respectively. For an $E1,M2$ mixing parameter x the lower limit to the $M2$ strength is greater than 20 for the $J=1$ solution $x=5.8$ and the $J=2$ solution $x=8.1_{-2.5}{}^{+6}$. Thus we conclude that these solutions are excluded if the 1.08-MeV level has odd parity. Also, the $J=1$ solution $x=0.17$ and the $J=2$ solution $x=-(0.23\pm0.07)$ both give a lower limit to the $M2$ strength of 0.5 Weisskopf units, and this value is improbably large, so that even parity is preferred if $J=1$ or 2.

In summary, the establishment of a $2.10\rightarrow1.08$ cascade and the lifetime limit, $\tau<10^{-8}$ sec, for the 1.08-MeV level together with previous work[9,11] allow a lifetime limit of $\tau<2\times10^{-10}$ sec to be set for the 1.08-MeV level. The angular distribution measurements on the F^{18} $1.08\rightarrow0$ transition allow $J=0$, 1 or 2 for the 1.08-MeV level with the mixing parameter x equal to $-(0.23\pm0.07)$ or $8.1_{-2.5}{}^{+6}$ for $J=2$ and all values of x allowed for $J=1$. However, the observation of isotropy for the $1.08\rightarrow0$ transition in two measurements in the present work and two measurements in previous work[11] rules against the solution $x=8.1_{-2.5}{}^{+6}$ for $J=2$ and for the solutions $x\simeq0.17$ or 5.80 for $J=1$. All four solutions for x for $J=1$ and 2 are seen to demand improbably large $M2$ transition strengths so that if $J=1$ or 2 we conclude that the parity is most probably even, with the preference for even parity stronger for $J=2$ than for $J=1$.

D. The 2.10-MeV Level

The (p,γ) correlation for the sixth-excited state at 2.10 MeV was measured at a bombarding energy of 4.0 MeV during the first series of measurements. Gamma-ray spectra were recorded at angles of 20, 35, 50, 65, and 90°. The sum of all the spectra with the randoms subtracted is shown in Fig. 11. The full-energy-loss peaks identified in Fig. 11 are assigned to the ground-state transition and cascades through the first and third excited states at 0.940 and 1.082 MeV. It is obvious that the $2.10\rightarrow0.940\rightarrow0$ cascade is present, but not so obvious that the peak near 1.05 MeV is composed of the 1.018-MeV, 1.082-MeV doublet from the $2.10\rightarrow1.082\rightarrow0$ cascade rather than the 1.055-MeV, 1.045-MeV doublet from the $2.10\rightarrow1.045\rightarrow0$ cascade. The evidence for the preference for the $2.10\rightarrow1.082\rightarrow0$ cascade was obtained by analyzing the pulse-height region between channels 36 and 62 with a least-squares Gaussian peak fitting program.[44] To begin with, three peaks were assumed and the full width at half-maximum of the highest energy peak was taken as 1.11 times that of the lowest energy peak. (This relationship arises from assuming an $E_\gamma{}^{1/2}$ dependence for the resolution of the NaI crystal.) The widths of the other two peaks and the energies and intensities of all three peaks were left as free parameters to be determined. Both exponential and straight line backgrounds were assumed. The results for these different backgrounds were found to differ negligibly except for the absolute areas in the peaks which differed by about 25%. The result of this fit was, using the 0.511-, 0.940-, and 2.10-MeV peaks for calibration, 1.050 ± 0.007 and 1.17 ± 0.01 MeV for the two higher energy peaks. The energy 1.17 ± 0.01 MeV, agrees with that expected for the $2.10\rightarrow0.940$ transition while the energy of the center peak agrees with the mean of a 1.018-MeV, 1.082-MeV doublet or the 1.045-MeV, 1.055-MeV doublet. More importantly, the width of the center peaks was found to be $(60\pm22)\%$ greater than expected for a 1.045-MeV, 1.055-MeV doublet but consistent with a 1.018-MeV, 1.082-MeV doublet. The next step was to assume four peaks with the positions of the 0.940- and 1.16-MeV peaks fixed and the widths of all four fixed from the $E_\gamma{}^{1/2}$ relationship as a constant times that of the 0.940-MeV peak. The positions of the middle two peaks and the intensities of all four were left as free parameters. The result of this fit is shown in Fig. 12 for the case of an exponential background. The energies of the central two peaks, based on 0.940 and 1.160 MeV for the other two peaks, were found to be 1.019 ± 0.004 and 1.079 ± 0.005 MeV, in good agreement with those expected for the 1.018-MeV, 1.082-MeV doublet but in disagreement with those expected for the 1.045, 1.055-MeV doublet. Thus

[44] P. McWilliams, W. S. Hall, and H. E. Wegner, Rev. Sci. Instr. **33**, 70 (1962).

the results of the Gaussian fittings to the summed spectra indicate that the 2.10-MeV level decays to the 0.940- and 1.082-MeV levels as well as to the ground state.

The branching ratios of the 2.10-MeV level were determined from the summed spectra using the results of the least-squares Gaussian fitting program. The intensities of the 0.940- and 1.16-MeV peaks and the 1.019- and 1.079-MeV peaks were found to be equal within the errors after correction for the dependence of crystal efficiency on gamma-ray energy. These intensities and that of the 2.10-MeV peak were combined to give branching ratios of $(38\pm3)\%$, $(28\pm5)\%$, and $(34\pm4)\%$ for the branches to the ground state, 0.940-MeV level, and 1.082-MeV level, respectively. Note that these results are given for the assumption that the $2.10 \rightarrow 1.045$ branch is neglibily small and, although the results are consistent with its absence, no sharp limit can be placed on the relative intensity of this branch. These branching ratios are in fair agreement with the previous work of Kuehner *et al.*[11] who found 30, 35, and 35%, respectively, for these three branches without determining to which of the two states at 1.045 and 1.082 MeV the latter branch belonged.

The angular distribution of the $2.10 \rightarrow 0$ transition was fitted to a Legendre polynomial expansion with the result $a_2 = -(0.27\pm0.08)$, $a_4 = +(0.04\pm0.10)$. The χ^2 computer fits to this distribution for spins of 2 and 3 are shown in Fig. 13. For $J=0$ and 1 the values of χ^2 are 4.8 and 0.32 [except near the roots of $F_2(11)$], respectively, so that $J=0$ is ruled out but $J=1$ is allowed for all values of x except those near the two roots of $F_2(11)$. The dashed curves given in Fig. 13 for $J=2$ and 3 illustrate the finite size effect. It is clear that $J=3$ is ruled against but that $J=2$ is allowed for two

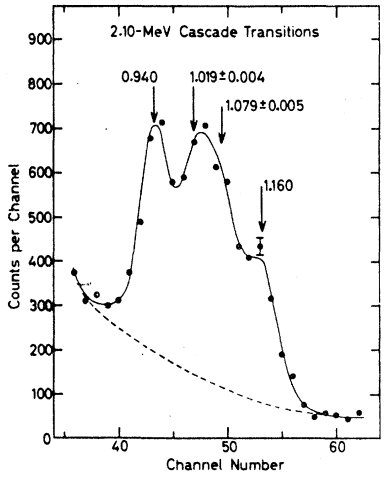

FIG. 12. Expanded plot of the 1-MeV complex of peaks observed from the decay of the F^{18} 2.10-MeV level. The closed circles are the sum of the seven spectra, including randoms, recorded at five angles to the beam. The solid curve is a least-squares fit (see text) to the points assuming four Gaussian peaks and an exponential background (broken curve).

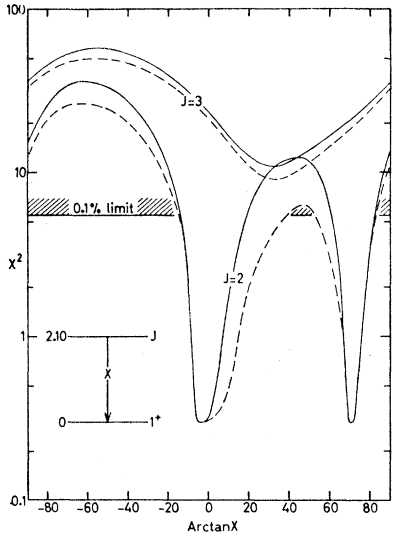

FIG. 13. χ^2 versus arctan x for the F^{18} $2.10 \rightarrow 0$ transition and assumed spins of 2 and 3 for the 2.10-MeV level. The full curves are for population of the $\alpha=0, \pm1$ magnetic substates only, while the broken curves are for $P(2)=0.1P(1)$.

regions of arctan x. The two regions of arctan x allowed for $J=2$ are $+(2\pm10)°$ and $+(72\pm3)°$, corresponding to $x=+(0.04\pm0.18)$ and $+(3.0\pm0.5)$. For $J=4$ and a pure octupole transition χ^2 is calculated to be 43.6, so that this situation is ruled out. Spins higher than 4 and a spin of 4 with significant admixtures of $L=4$ radiation are eliminated by the lifetime limit $\tau<10^{-8}$ sec since, for example, this limit would correspond to a speed for $E4$ radiation of $5\times10^6x^2/(1+x^2)$ times the Weisskopf estimate where x^2 is the intensity ratio of $E4$ to $M3$ radiation

The angular distributions of the gamma rays from the cascades from the 2.10-MeV level to the 0.94- and 1.08-MeV levels were obtained from the Gaussian least-squares fits to the gamma-ray spectra. An attempt was made to gain some information from these angular distributions. However, the uncertainties resulting from separating the three peaks shown in Figs. 11 and 12 were so large that these angular distributions gave no useful information and this attempt failed.

To summarize the present results, we find that the 2.10-MeV level decays to the F^{18} ground state, 0.94- and 1.08-MeV levels with branches of (38 ± 3), (28 ± 5), and $(34\pm4)\%$. Analysis of the angular distribution of the $2.10 \rightarrow 0$ transition rules out spin assignment to the 2.10-MeV level of $J=0$ and $J\geq3$. Both $J=1$ and 2 are allowed by the present results with $x=+(0.04\pm0.18)$ or (3.0 ± 0.5) for $J=2$.

We now consider the consequences of the lifetime measurement[10] of $(0.7\pm0.2)\times10^{-12}$ sec for the 2.10-MeV level on the spin-parity assignments for the 2.10- and 1.08-MeV levels. The quadrupole strengths of the transition from the 2.10-MeV level to the F^{18} ground state, 0.94- and 1.08-MeV levels obtained from the lifetime measurement[10] and our branching ratio meas-

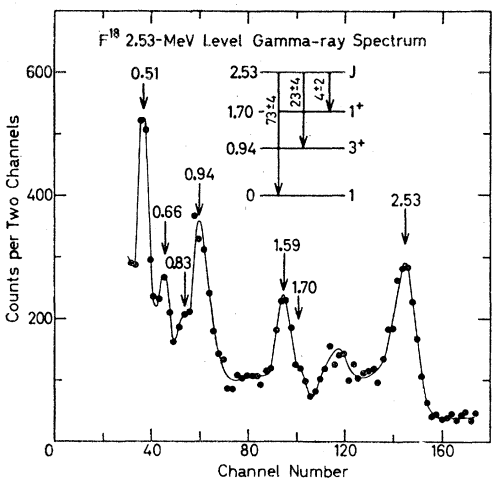

FIG. 14. Spectrum of gamma rays in coincidence with the proton group populating the F^{18} 2.53-MeV level in the $O^{16}(He^3,p)F^{18}$ reaction at a He^3 energy of 4.0 MeV. The positions of the gamma-ray peaks expected from the inserted decay scheme are indicated by the arrows. The spectrum is the sum of ten spectra recorded at five angles to the beam. The randoms have been subtracted.

urements are given in Table VII. From this table we see that the consequences of the lifetime measurement for the 2.10-MeV level are: (1) An assignment of $J^\pi=1^-$ for the 2.10-MeV level is ruled out by the $M2$ strength of the transition to the $J^\pi=3^+$, 0.94-MeV level, and an assignment of $J^\pi=1^+$ is unlikely because of the $E2$ strength of this transition. (2) If the 2.10-MeV level has $J^\pi=2^-$ then the solution $x=+(3.0\pm0.5)$ is ruled out for the $2.10\rightarrow0$ transition, the 1.08-MeV level is not $J^\pi=0^+$, and $J^\pi=0^-$ is quite unlikely. (3) If the 2.10-MeV level has $J^\pi=2^+$ then the 1.08-MeV level is not $J^\pi=0^-$, and $J^\pi=0^+$ is quite unlikely. Thus, we find from the evidence considered here that the 2.10-MeV level is most probably $J=2$, with $J^\pi=1^+$ another possibility, while the 1.08-MeV level is most probably $J=1$ or 2.[45] The conclusion reached here that the 1.08-MeV level is probably not $J=0$ and if $J=1$ or 2 probably has even parity appears to disagree with previous results from the $N^{14}(\alpha,\gamma)F^{18}$ reaction of Price[46] and of Almqvist *et al.*[47] Thus we shall quote $J=0$, 1, 2 for this level and shall not indicate a preference of $J=2$ over $J^\pi=1^+$ for the 2.10-MeV level.

TABLE VII. Quadrupole strengths in Weisskopf units for the decay of the F^{18} 2.10-MeV level.

Final state (MeV)	$E2$	$M2$
0	3.4 ± 1.2^a	77 ± 23^a
0.94	54 ± 18	$(1.2\pm0.4)\times10^3$
1.08	128 ± 42	$(2.8\pm1.1)\times10^3$

[a] For $J=2$, $x=(3.0\pm0.5)$.

[45] A roughly similar conclusion was reached by Litherland *et al.* (Ref. 10). However, these authors imply ~150 $E2$ Weisskopf units for the $2.10\rightarrow0.94$ transition while we obtain 54 ± 18; thus we do not find as strong a rejection of $J^\pi=1^+$ for the 2.10-MeV level and therefore $J=0$ for the 1.08-MeV level.

[46] P. C. Price, Proc. Phys. Soc. (London) **A68**, 553 (1955).

E. The 2.53-MeV Level

The decay of the 2.53-MeV level was studied during the second series of measurements at a bombarding energy of 4.0 MeV. Spectra were recorded at angles of 0, 30, 45, 65, and 90°. The sum of all ten spectra recorded is shown in Fig. 14. For the kinematics involved, the proton group leading to the N^{14} 4.91-MeV level following the $C^{12}(He^3,p)N^{14}$ reaction was unresolved from the proton group feeding the F^{18} 2.53-MeV level (see Fig. 1). The N^{14} 4.91-MeV level decays 100% by a ground-state transition.[8] The counts above channel 155 in Fig. 14 are due to this transition. The presence of this 4.91-MeV gamma ray was not a serious complication since its contribution to the pulse-height region of interest could be readily subtracted. The full-energy-loss and one-escape peaks of a 2.53-MeV gamma ray from the $2.53\rightarrow0$ transition are apparent in Fig. 14. In addition, gamma rays of 1.59 and 0.94 MeV from the cascade $2.53\rightarrow0.94\rightarrow0$ can also be recognized. There also appears to be a 0.66-MeV gamma ray and gamma rays of 0.83 and 1.70 MeV which are not resolved from the more intense peaks at 0.94 and 1.59 MeV may be present. These gamma rays would result from a transition to the 1.70-MeV level. Branching ratios obtained from these ten spectra are $(73\pm4)\%$, $(23\pm2)\%$, and $(4\pm2)\%$ for decay of the 2.53-MeV level to the F^{18} ground state and the 0.94- and 1.70-MeV levels, respectively. These branching ratios are in fair agreement with the previous work of Kuehner *et al.*[11] who found 79, 18, and <3%, respectively, for these three branches.

The angular distribution of the $2.53\rightarrow0$ transition was analyzed to give $a_2=-(0.12\pm0.05)$, $a_4=-(0.37\pm0.05)$. The χ^2 fits to this distribution for $J=2$

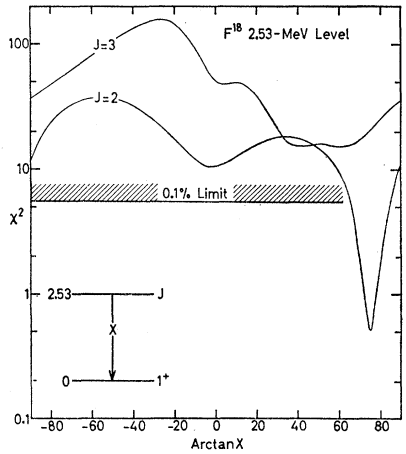

FIG. 15. χ^2 versus arctan x for the F^{18} $2.53\rightarrow0$ transition and assumed spins of 2 and 3 for the 2.53-MeV level.

[47] E. Almqvist, D. A. Bromley, and J. A. Kuehner, Bull. Am. Phys. Soc. 3, 27 (1958).

and 3 are shown in Fig. 15. A spin assignment of 0 is ruled out by the nonisotropic distribution. An assignment of $J=1$ is ruled out by the nonzero value of a_4. For $J=4$ with pure $L=3$ radiation $\chi^2=105$ so that this situation is not allowed. As in the case of the $2.10 \rightarrow 0$ transition, $J=4$ with appreciable mixtures of $L=4$ radiation and $J=5$ or higher are improbable because of the lifetime limit, $\tau<10^{-8}$ sec. For example, this limit would correspond to a matrix element for $E4$ radiation of $10^6x^2/(1+x^2)$ times the Weisskopf estimate if $J=4$.

It is seen from Fig. 15 that the assignment $J=3$ is in disagreement with the measured distribution, while the χ^2 plot for $J=2$ has one solution, arctan $x=74\pm4°$ ($x=3.5_{-0.75}{}^{+1.2}$). The finite size effect was investigated and found to have negligible effect on the $J=2$ curve. The $J=3$ curve, although affected quite appreciably, does not come down below the 0.1% limit when this effect is estimated by setting $P(2)=0.1P(1)$.

The angular distributions of the 1.59- and 0.94-MeV gamma rays from the $2.53 \rightarrow 0.94 \rightarrow 0$ cascade were also analyzed. The results are $a_2=-(0.17\pm0.12)$, $a_4=-(0.12\pm0.19)$ for the 1.59-MeV gamma ray and $a_2=+(0.12\pm0.07)$, $a_4=+(0.08\pm0.09)$ for the 0.94-MeV gamma ray. Two gamma-ray χ^2 fits were made to these two distributions with $J=3$ for the 0.94-MeV level and $x=0$ for the $0.94 \rightarrow 0$ transition, and varying the mixing parameter for the $2.53 \rightarrow 0.94$ transition. Also, three gamma-ray χ^2 fits were made by including the $2.53 \rightarrow 0$ transition with these two and fixing the mixing parameter for this transition at the minimum shown in Fig. 14. When the finite size effect was included, there was very little dependence of χ^2 on the mixing parameter for the $2.53 \rightarrow 0.94$ transition. Thus this analysis gave no useful information.

To summarize the results of these measurements, the F^{18} 2.53-MeV level was found to decay to the ground state, the 0.94-MeV level and probably to the 1.70-MeV level with branches of (73±4)%, (23±2)%, and (4±2)%, respectively. The spin of the 2.53-MeV level was uniquely determined to be $J=2$ and the mixing parameter of the $2.53 \rightarrow 0$ transition was found to be $x=3.5_{-0.75}{}^{+1.2}$. Analysis of the angular distributions of the two members of the $2.53 \rightarrow 0.94 \rightarrow 0$ cascade gave no useful information on the mixing parameter for the $2.53 \rightarrow 0.94$ transition.

The lifetime of the 2.53-MeV level has been measured to be $(1.1\pm0.2)\times10^{-12}$ sec.[10] Combining this value with our measurements of the $2.53 \rightarrow 0$ branching ratio and the quadrupole-dipole mixing ratio for this $\Delta T=0$ transition gives 38±8 Weisskopf units for the $M2$ transition strength if the 2.53-MeV level were $J^\pi=2^-$. Thus we assign even parity to this level (see Sec. IIIC) in agreement with results[13] obtained from the $F^{19}(d,t)F^{18}$ reaction.

F. The 3.13-MeV Level

The proton groups forming the 3.06- and 3.13-MeV levels were not resolved (Fig. 1). However, a bombarding energy (3.65 MeV) was found at which there was no discernible population of the 3.06-MeV level. The 3.13-MeV level was studied at this bombarding energy with a proton gate set to exclude the major part of the pulse height region where the proton group feeding the 3.06-MeV level would lie. It is estimated that the contribution of the 3.06-MeV level to the gamma-ray spectra is at most 5% of that due to the 3.13-MeV level and has negligible effect on the results obtained for the latter level. Seven gamma-ray spectra were recorded at five angles during the second series of measurements. The sum of five of these spectra is shown in Fig. 15. It is clear from this figure that the 3.13-MeV level decays predominantly to the 1.045-MeV level with a weaker ground state branch. The branching ratios were found to be (69±4)% and (31±3)%, respectively, for the $3.13 \rightarrow 1.04$ and $3.13 \rightarrow 0$ transitions.

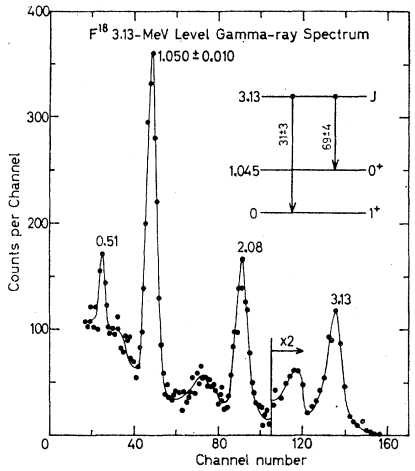

FIG. 16. Spectrum of gamma rays in coincidence with the proton group populating the F^{18} 3.13-MeV level in the $O^{16}(He^3,p)F^{18}$ reaction at an He^3 energy of 3.65 MeV. The spectrum is the sum of seven spectra recorded at five angles to the beam. The randoms have been subtracted. The decay scheme obtained from analysis of these spectra is also shown.

The results of the angular distribution measurements were $a_2=+(0.007\pm0.045)$, $-(0.68\pm0.05)$, and $+(0.29\pm0.08)$, respectively, for the gamma rays at 1.045, 2.085, and 3.13 MeV. There was no evidence for terms in $P_4(\cos\theta)$ for any of these distributions. These distributions are characteristic of the decay of a $J=1$ level to the $J=1$ ground state and $J=0$ 1.045-MeV level as was the case for the 1.70-MeV level; and, as can be seen from the two distribution χ^2 computer fits shown in Fig. 17, $J=1$ is allowed and $J=2$ and 3 are excluded by these distributions. Spin assignments of 4 or higher are excluded by the lifetime limit, $\tau<10^{-8}$ sec together with the branching ratio of the $3.13 \rightarrow 1.04$ transition, and $J=0$ is excluded by the $3.13 \rightarrow 1.045$ transition.

In summary, the 3.13-MeV level decays to the F^{18} ground state and 1.045-MeV level with branches of (31±3)% and (69±4)%, respectively. A unique as-

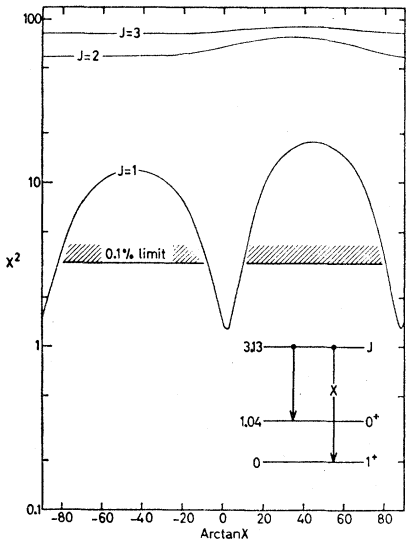

FIG. 17. χ^2 versus arctan x for the decay of the F^{18} 3.13-MeV level at $E_{He^3}=3.65$ MeV. The $3.13 \rightarrow 1.04$ and $3.13 \rightarrow 0$ angular distributions are fitted simultaneously as a function of the $(L+1)/L$ amplitude ratio, x, for the $3.13 \rightarrow 0$ transition. Curves are shown assuming $J=1$, 2, and 3 for the 3.13-MeV level.

signment of $J=1$ can be made to the 3.13-MeV level and the mixing parameter for the $3.13 \rightarrow 0$ transition is given by $x=+(0.03\pm0.04)$ or $|x|>10$.

G. The 3.06-MeV Level

The decay of the 3.06-MeV level was studied at a bombarding energy of 4.15-MeV with the proton gate set to include the proton groups leading to both the 3.06- and 3.13-MeV levels. The relative intensities of the two proton groups were determined using the least-squares Gaussian fitting program[44] mentioned earlier. The relative contributions of p_8 and p_9 to the doublet at $E_{He^3}=4.15$ MeV were 63 and 37%, respectively. Ten spectra were recorded at five angles during the second series of measurements. The sum of the ten spectra is shown in Fig. 18. It is clear from this figure that the 3.06-MeV level decays to the F^{18} ground state and 0.94-MeV level. The presence of a 1.045-MeV gamma ray from the $3.13 \rightarrow 1.045 \rightarrow 0$ cascade is also apparent and the 2.12- and 3.06-MeV peaks must contain contributions from the $3.13 \rightarrow 1.045$ and $3.13 \rightarrow 0$ transitions. The branching ratios of the 3.06-MeV level decay were determined from the spectrum of Fig. 18 after subtraction of the 37% contribution from the decay of the 3.13-MeV level. The evidence for a peak at 1.045 MeV which is seen in Fig. 18 was not apparent in the subtracted spectrum.

The branching ratios resulting from the present work are indicated in Fig. 18. These results are in good agreement with previous work. Almqvist, Bromley, and Kuehner,[47] using the $N^{14}(\alpha,\gamma)F^{18}$ reaction, obtained 80% and 20% for the decay of the 3.06-MeV level to the F^{18} ground state and 0.94-MeV level, while Kuehner *et al.*[11] obtained 25% for the relative intensity of the ground-state decay of the unresolved 3.13-3.06 doublet with the remaining 75% being due to decay to the F^{18} states near 1 MeV.[48]

Because of the presence of gamma rays from the 3.13-MeV level, the present results are not well suited to a determination of the spin of the 3.06-MeV level or a determination of the mixing parameters for its decay modes. However, some information can be obtained from these measurements. The angular distribution of the 0.94-MeV gamma ray from the $3.06 \rightarrow 0.94 \rightarrow 0$

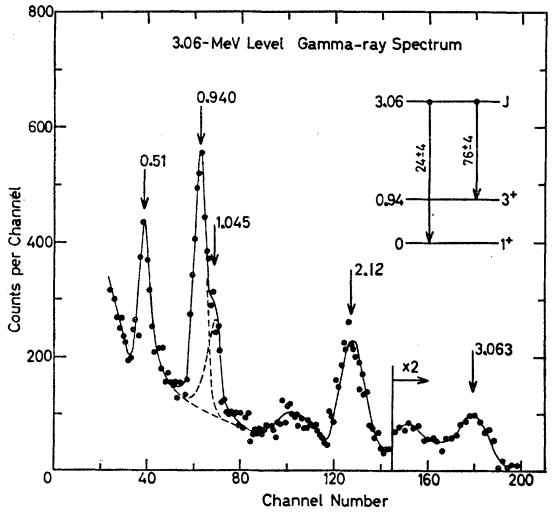

FIG. 18. Spectrum of gamma rays in coincidence with the proton groups populating the F^{18} 3.06- and 3.13-MeV levels in the $O^{16}(He^3,p)F^{18}$ reaction at a He^3 energy of 4.15 MeV. The relative intensities of these two proton groups was in the ratio 63:37. The spectrum is the sum of ten spectra recorded at five angles to the beam. The randoms have been subtracted. The decay scheme for the 3.06-MeV level resulting from analysis of these spectra is shown by the insert. This decay scheme was obtained after subtraction of the gamma-ray spectrum from the decay of the 3.13-MeV level (Fig. 16).

transition is the only one which can be straightforwardly extracted from the (p,γ) coincidence data and was the only one which was analyzed. The 0.94- and 1.045-MeV peaks were unresolved; however, the contribution of the 1.04-MeV peaks could easily be subtracted since the $1.045 \rightarrow 0$ transition is isotropic by virtue of the zero spin of the 1.045-MeV level. Analysis of the angular distribution of the 0.94-MeV transition gave $a_2=+(0.32\pm0.08)$, $a_4=-(0.17\pm0.07)$. Computer fits were made to this distribution assuming $J=0$, 1, 2, and 3 for the 3.06-MeV level and $J=3$ for the 0.94-MeV level. The mixing parameter for the $0.94 \rightarrow 0$ transition was fixed at zero and the mixing parameter for the $3.06 \rightarrow 0.94$ transition was varied. The results are shown in Fig. 19. The 0.1% limit for these fits is at $\chi^2=5.5$, just

[48] Kuehner *et al.* (Ref. 11) associate this 75% branch with decay to the 0.94-MeV level. However, it appears from their published spectra that this branch can be partially to the 1.045-MeV level as well.

above the value for $J=0$. The finite size effect was negligible. The present results favor an assignment of $J=2$ for the 3.06-MeV level. However, $J=3$ and $J=1$ are only ruled against with 80% and 85% confidence, respectively, so that $J=2$, 3 and 1 are all possible assignments with relative likelihoods in the ratio 3.3:1.3:1, respectively. If $J=2$, then the mixing parameter for the $3.06 \rightarrow 0.94$ transition has the 85% confidence limit $x^2 \leq 1$. Spin assignments of $J=4$ or higher were not considered. They are not allowed by the $N^{14}(\alpha,\gamma)F^{18}$ results of Price[46] and Almqvist *et al.*[47]

In summary, the 3.06-MeV level was found to decay to the F^{18} ground state and 0.94-MeV level with branching ratios of (24 ± 4)% and (76 ± 4)%, respectively. The 3.06-MeV level can have $J=1$, 2, or 3 with the likelihood of $J=2$, 3 and 1 in the ratio 3.3:1.3:1. If $J=2$, then the $3.06 \rightarrow 0.94$ transition has the 85% confidence limit $x^2<1$.

H. The 3.35-MeV Level

Gamma-ray spectra in coincidence with the proton group feeding the F^{18} 3.35-MeV level were recorded in the second series of measurements at a bombarding

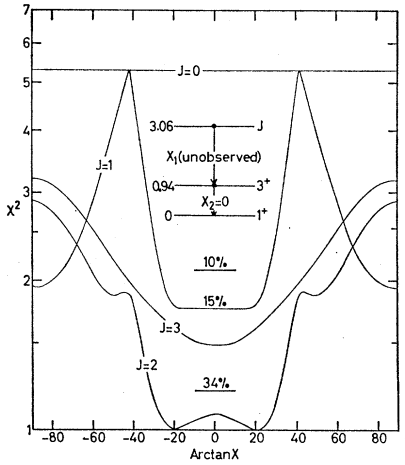

FIG. 19. χ^2 versus arctan x for the second transition in the F^{18} $3.06 \rightarrow 0.94 \rightarrow 0$ cascade with the mixing ratio x_2 of the $0.94 \rightarrow 0$ transition fixed at zero and the mixing ratio x_1 of the $3.06 \rightarrow 0.94$ transition variable. Curves are shown assuming $J=0$, 1, 2, and 3 for the 3.06-MeV level. The percentages indicated give the probability that a correct solution has a χ^2 of the corresponding value or larger.

energy of 4.0 MeV. Spectra were taken at 0, 30, 45, 65, and 90° to the beam on two successive days. On the first day seven spectra were recorded while on the second day six were recorded. The sum of all 13 spectra is shown in Fig. 20. The full-energy-loss and one-escape peaks of a $3.35 \rightarrow 0$ transition are apparent in this figure as well as the 0.66- and 1.045-MeV gamma rays characteristic of the decay of the 1.70-MeV level. The 1.67-MeV peak is composed mostly of the 1.65-MeV gamma ray from the $3.35 \rightarrow 1.70$ transtion with a contribution from the $1.70 \rightarrow 0$ transition. Thus the 3.35-MeV level decays predominantly to the ground state and 1.70-MeV level. Other gamma rays apparent in the spectrum of Fig. 20 are 0.51-MeV annihilation radiation and weak gamma rays of (1.25 ± 0.08) and (2.34 ± 0.06) MeV. The former probably arises from a $3.35 \rightarrow 2.10$ transition. The gamma-ray peaks associated with the transitions from the 2.10-MeV level would be unresolved from nearby peaks of greater intensity and would not be expected to show up. The 2.34-MeV peak is partially due to the two-escape peak of the 3.35-MeV gamma ray and may contain a contribution from the 2.41-MeV gamma ray expected from the $3.35 \rightarrow 0.94$ transition. However, it was shown to be mostly due to the 2.31-MeV gamma ray from the N^{14} $5.69 \rightarrow 2.31 \rightarrow 0$ cascade. This gamma ray and gamma rays of 3.38 and 6.59 MeV are present since the proton group from the $C^{12}(He^3,p)N^{14}$ (5.69-MeV level) reaction is unresolved from that feeding the F^{18} 3.35-MeV level (see Fig. 1).

The contribution of gamma rays from the decay of the N^{14} 5.69-MeV level was subtracted from the individual spectra using the known[8,23] decay modes of this level, the known mixing ratio for the N^{14} $5.69 \rightarrow 0$ transition,[23] and the intensity of that part of the 5.69-MeV gamma-ray spectrum appearing between channels 210 and 256. A spectrum taken at one-half the gain was of use in making this subtraction. This spectrum was taken using a target with six times the carbon contamination of that used to obtain the angular distributions on the first day of measurements. The carbon contamination was monitored during the measurements by continuous observation of the relative intensity of the proton peak feeding the N^{14} 5.10-MeV

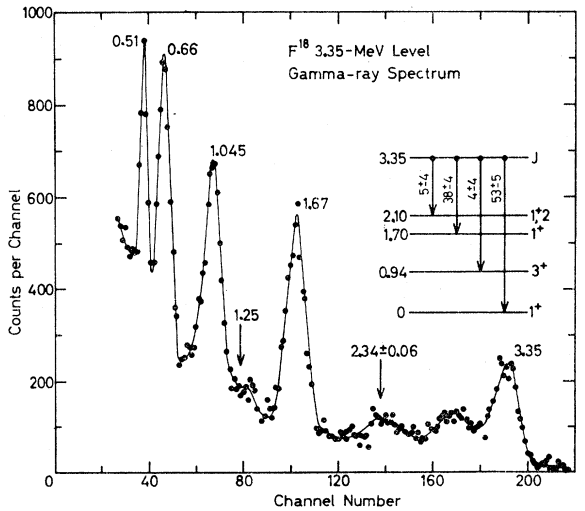

FIG. 20. Spectrum of gamma rays in coincidence with the proton group populating the F^{18} 3.35-MeV level in the $O^{16}(He^3,p)F^{18}$ reaction at an He^3 energy of 4.0 MeV. The spectrum is the sum of 13 spectra recorded at five angles to the beam. The randoms have been subtracted. The decay scheme resulting from analysis of these spectra is also shown.

level (N^{14} p_4 in Fig. 1). The amount of carbon contaminant on the second day of running was roughly double that for the first day. The branching ratios obtained from the 13 spectra were (53±5), (4±4), (38±4), and (5±4)%; for decay to the F^{18} ground state, 0.94-, 1.70-, and 2.10-MeV levels, respectively. Gamma-ray cascades from this level have not been observed previously.

The angular distribution of the 3.35 → 0 transition was analyzed after subtraction of the contribution of the 3.38-MeV gamma ray from the N^{14} 5.69 → 2.31 transition. The analysis gave $a_2=+(0.47\pm0.06)$, $a_4=-(0.27\pm0.07)$. The χ^2 computer fits to this distribution for $J=0$, 1, 2, and 3 are shown in Fig. 21. The 0.1% limit for this figure is at 5.3, just below the χ^2 curve for $J=1$. It is clear that $J=0$ and 1 are ruled out, but that there are solutions for x for both $J=2$ and 3. For $J=4$ with pure $L=3$ radiation, $\chi^2=16$. The lifetime limit $\tau<10^{-8}$ sec combined with the 3.35 → 0 branching ratio gives lower limits for $E4$ and $M4$ matrix elements of $4.3\times10^4\,x^2/(1+x^2)$ and $1.8\times10^6\,x^2/(1+x^2)$, respectively, times the Weisskopf estimate. Thus significant deviations of x from 0 (i.e., arctan $x\geq5°$) are not possible and spin assignments of 4 or higher are excluded. The finite size effect was found to have very little effect on the χ^2 curve for $J=3$, but for $J=2$ the two minima were merged together. The values of arctan x, for $J=3$ at the two minima shown in Fig. 21, are (1±3)° and (76±3)°, corresponding to values for x of (0.02±0.05) and $4_{-0.75}{}^{+1.1}$. For $J=2$ the limits on arctan x are $-78°\leq\arctan x\leq-40°$, corresponding to $-4.7\leq x\leq-0.8$.

The angular distributions of the 1.67- and 0.66-MeV peaks were also analyzed. The results were $a_2=+(0.18\pm0.06)$, $a_4=-(0.13\pm0.07)$ for the 1.67-MeV peak and $a_2=-(0.38\pm0.07)$ for the 0.66-MeV peak. Two distribution χ^2 computer fits were made to the angular distribution of these two peaks for assignments to the 3.35-MeV level of $J=2$ and 3. In each case the mixing parameter of the 3.35 → 1.70 transition was varied, since the 0.66-MeV transition from the $J=1$, 1.70-MeV level to the $J=0$, 1.04-MeV level is pure. A complication in this analysis is that the 1.67-MeV peak has a contribution from the 1.70 → 0 transition as well as from the 1.65-MeV 3.35 → 1.70 transition. However, the (p,γ) correlation measurements for the decay of the 1.70-MeV level gave the branching ratio (35%) and determined the value of the function $F_2(11)$ for the 1.70 → 0 transition. Using these experimental data, the presence of the 1.70-MeV gamma ray can be taken account of by a straightforward modification of the theoretical formulae describing the 3.35 → 1.70 transition. This could be done without introducing much additional error since the 1.70-MeV (1.70 → 0) gamma ray is only 0.35% as intense as the 1.65-MeV (3.35 → 1.70) gamma ray. The results of these two-distribution χ^2 fits were found to be sufficiently informative to warrant additional analysis, so a three-distribution χ^2 fit was made by including the distribution for the 3.35 → 0 transition. This was done to ensure that the population parameters for the two decay modes, 3.35 → 0 and 3.35 → 1.70, were consistent with each other. In this analysis the mixing parameter for the 3.35 → 0 transition was fixed at the values given by the minima shown in Fig. 21. For $J=3$, fits were made for values of 0° and 76° for arctan x, where x applies to the 3.35 → 0 transition. For $J=2$, fits were made at four values of arctan x between the experimentally determined limits of −78° and −40°. For both spin values the χ^2 curves for the different values of

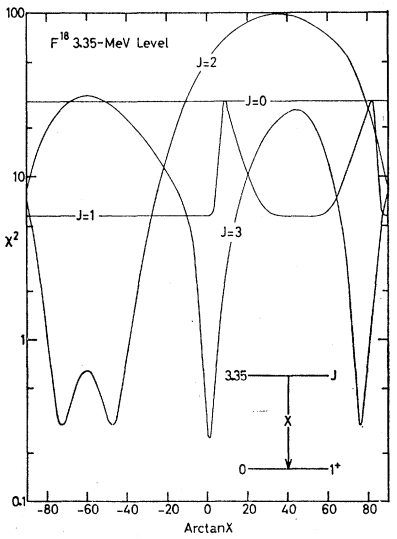

FIG. 21. χ^2 versus arctan x for the F^{18} 3.35 → 0 transition and assumed spins of 0, 1, 2 and 3 for the 3.35-MeV level.

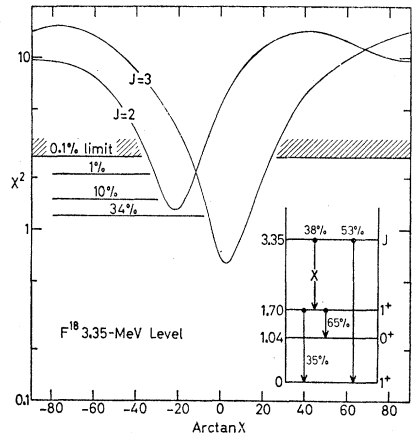

FIG. 22. χ^2 versus arctan x for the decay of the F^{18} 3.35-MeV level to the ground state and through the 1.70-MeV level. The sum of the 3.35 → 1.70 and 1.70 → 0 transitions, the 3.35 → 0 transition and the 1.70 → 1.04 transition were fitted simultaneously as a function of the $(L+1)/L$ amplitude ratio x for the 3.35 → 1.70 transition. Curves are shown assuming pure quadrupole radiation for the 3.35 → 0 transition and $J=2$ and 3 for the spin of the 3.35-MeV level. The percentages indicated give the probability that a correct solution has a χ^2 of the corresponding value or larger.

arctan x were found to differ negligibly and were also found to be almost identical with the χ^2 curves obtained from the two distribution fits. Results for one of the three-distribution fits for both $J=2$ and $J=3$ are shown in Fig. 22. From these curves we find that both $J=2$ and $J=3$ are possible spin assignments for the 3.35-MeV level but that $J=3$ is twice as likely as $J=2$. For $J=3$ the minimum corresponds to arctan $x=(3\pm7)°$, while the minimum for $J=2$ corresponds to arctan $x=-(22\pm7)°$, where x is the mixing parameter for the $3.35\rightarrow1.70$ transition. These values of arctan x correspond to values for x of $+(0.05\pm0.12)$ and $-(0.40\pm0.15)$, respectively.

In summary, the 3.35-MeV level was found to decay to the ground state, 0.94-, 1.70-, and 2.10-MeV levels with branching ratios of (53±5), (4±4), (38±4), and (5±4)%, respectively. The spin of the 3.35-MeV level is $J=2$ or 3, with 3 more probable than 2. If $J=3$ then the mixing parameter of the $3.35\rightarrow0$ transition is $+(0.02\pm0.05)$ or $4_{-0.75}^{+1.1}$ and for the $3.35\rightarrow1.70$ transition it is $+(0.05\pm0.12)$. If $J=2$, then the mixing parameter of the $3.35\rightarrow0$ transition is in the range $-4.7\leq x\leq-0.8$ and for the $3.35\rightarrow1.70$ transition it is $-(0.40\pm0.15)$. We note that the relative strength of the quadrupole transitions to the $J^\pi=1^+$ ground state and 1.70-MeV level compared to the other possible decay modes would seem most reasonable if the 3.35-MeV level were $J^\pi=2^+$, and that they would appear to be quite difficult to understand if the 3.35-MeV level had odd parity. Because of this argument and the slight preference for $J=3$ over $J=2$ obtained in the (p,γ) work we quote $J=2$ or 3 for this level and do not retain the preference for 2^- which would be indicated by the rather inconclusive $F^{19}(p,d)F^{18}$ and $F^{19}(d,t)F^{18}$ results.[13,15]

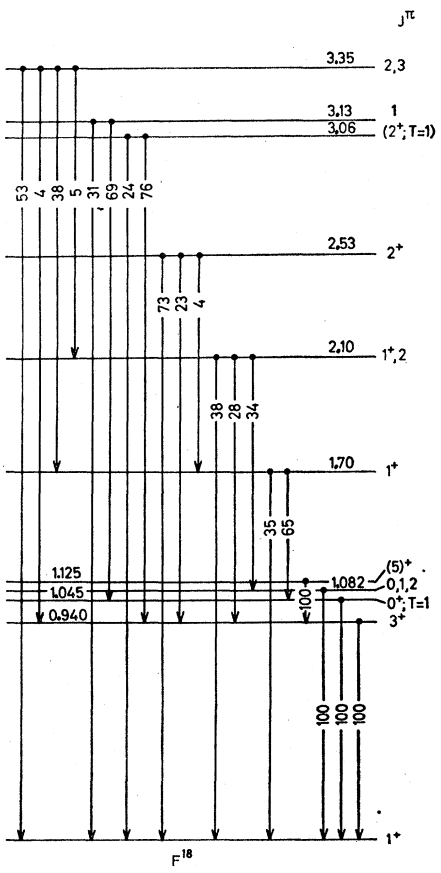

FIG. 23. Summary of the gamma-ray de-excitation branching ratio measurements from the present work and spin-parity assignments resulting from this and previous work. The $T=1$ levels are indicated, all other levels are expected to have $T=0$.

V. DISCUSSION AND COMPARISON WITH THEORY

The decay scheme of F^{18} resulting from the evidence presented in Sec. IV and from previous work[8] is shown in Fig. 23. The branching ratios given in this figure, which are taken from the present work, are all consistent with previous measurements[8,11] as are the indicated spin assignments.

We now wish to compare the experimental results with the theoretical predictions. To begin, we attempt to identify the states which belong predominantly to the group of states formed by two particles in the $2s_{1/2}$, $1d_{5/2}$, and $1d_{3/2}$ shells with the $1s$ and $1p$ shells closed at O^{16}. We shall call this group of states the $(2s,1d)^2$ configuration. The various theoretical predictions for the excitation energies of these states[1–5] are in quite good agreement. These calculations are all consistent with an identification of the F^{18} ground state, 0.94-MeV level, and 1.125-MeV level with the lowest $J^\pi=1^+$, 3^+, and 5^+ states of the $T=0$ spectrum, and an identification of the 1.045- and 3.063-MeV levels with the lowest 0^+ and 2^+ $T=1$ states. All the known properties of these states are consistent with these assignments[5] and the present work strengthens them since we have confirmed the suspected $J^\pi=3^+$ nature of the 0.940-MeV level. Furthermore, the assignment of $J=1$ to the 3.13-MeV level removes the only contender other than the 3.06-MeV level for the $J^\pi=2^+$, $T=1$ analog of the first-excited state of O^{18} at 1.98 MeV.[8]

No other $T=1$ levels are expected at excitation energies below about 4.6 MeV, this being the energy at which the analog of the O^{18} second-excited state is predicted. However, three additional $T=0$ levels with $J^\pi=1^+$, 2^+, and 3^+ are predicted within the approximate range 2.5–5 MeV above the ground state. The ordering, as well as the excitation energies, of these levels appears to depend rather sensitively on the details of the model and so is not predicted with great accuracy. Flowers and Wilmore[5] attempted to identify these states with the known levels of F^{18} using mainly their predictoins for the strengths of the $M1$ and $E2$ transitions connecting them with the F^{18} ground state and the 0.94- and 1.045-MeV levels. They made a tentative identification of the $J^\pi=1^+$ state with the 1.70-MeV level and the $J^\pi=2^+$ state with the 2.10-MeV level or possibly the 2.53-MeV

TABLE VIII. The transition strengths in Weisskopf units for the decay of the F^{18} 2.10- and 2.53-MeV levels (both assumed to have even parity) to the ground state and 0.940-MeV level. The theoretical predictions for the transitions from the first $J^\pi=2^+$ level of $(2s,1d)^2$ are also shown.

Initial state	2.10-MeV level		2.53-MeV level		Theory (2^+ level)[c]	
Final state	$M1$	$E2$	$M1$	$E2$	$M1$	$E2$
Ground	$(18\pm5)\times10^{-4}$[a] $(1.8\pm0.7)\times10^{-4}$[b]	≤0.24[a] 3.4 ± 1.2[b]	$(1.0\pm0.5)\times10^{-4}$	1.7 ± 0.4	3.9×10^{-4}	7.0
0.94-MeV level	$(0-11)\times10^{-3}$	72−0	$(0-2)\times10^{-3}$	6−0	$(4-10)\times10^{-3}$	9.5

[a] $x=+(0.04\pm0.18)$. [b] $x=+(3.0\pm0.5)$. [c] Flowers and Wilmore, Ref. 5.

level. They concluded that neither the 2.10- or 2.53-MeV levels could easily be identified with the 3^+ state since its ground-state transition is predicted to be very slow. The present results confirm this latter conclusion since neither level can have $J=3$.

The lowest known level of F^{18} that can be the second $J=3$ level is the one at 3.35 MeV. However, its decay modes are in severe disagreement with the predictions of Flowers and Wilmore for the 3^+ state in question. The predicted intensity ratio of the branches to the ground state and 0.940-MeV level if the 3.35-MeV level is this 3^+ state is[5] $(1.9\pm0.4):100$, while the experimentally observed ratio is $(53\pm5):(4\pm4)$. Furthermore, the $(38\pm4)\%$ branch to the 1.70-MeV level is an order of magnitude or more larger than predicted if the 1.70-MeV level is the second 1^+ state of $(2s,1d)^2$ as suspected.[49] Thus we conclude that the second 3^+ level of $(2s,1d)^2$ most probably lies above an excitation energy of 3.5 MeV.

The candidates for the second $T=0$, $J^\pi=1^+$ level of $(2s,1d)^2$ are the states at 1.70 and 3.13 MeV while the candidates for the 2^+ state are the 2.10-, 2.53-, and 3.35-MeV levels. The 1.08-MeV level appears to be of too low an excitation to be associated with either state. Also the 1.08-MeV level is quite weakly excited and shows no stripping pattern in the $O^{16}(He^3,p)F^{18}$ reaction,[50] which is inconsistent with the expected behavior for the 1^+ and 2^+ states of $(2s,1d)^2$. Flowers and Wilmore[5] found that the strengths of the transitions from the 1.70-MeV level are consistent with their predictions. With the additional information provided by our work we find this still to be true. Using our branching ratios and the lifetime measurement of Litherland *et al.*[10] the $1.70\rightarrow1.045$ transition has an $M1$ strength of $(3.5\pm1.8)\times10^{-2}$ Weisskopf units while the predicted strength is $\approx5.2\times10^{-2}$ Weisskopf units for the favored parameters of the calculation. Using the two possible values of the $M1,E2$ mixing ratio found for the $1.70\rightarrow0$ transition, (0.49 ± 0.06) and (2.05 ± 0.3), we find strengths for this transition of 9×10^{-4} or 2×10^{-4} for $M1$ and 0.66 or 2.8 for $E2$, all with 50% uncertainty. The predicted strengths are $(7-30)\times10^{-4}$ and 1.14 Weisskopf units for $M1$ and $E2$, respectively. Thus the $M1$ and $E2$ strengths of the $1.70\rightarrow0$ transition, as well as the $M1$ strength of the $1.70\rightarrow1.045$ transition, are in rather good agreement with those predicted for the second 1^+ state especially for $x=+(0.49\pm0.06)$.[51] However, the decay modes of the 3.13-MeV level and the solution $|x|>10$ for the mixing parameter of the $3.13\rightarrow0$ transition are also consistent with the theoretical predictions[5] for the second 1^+ state. Thus, it appears likely that one of these two levels is the second 1^+ state, but it does not appear possible to make a definite choice between them on the basis of the available experimental information.

The transition strengths of the F^{18} 2.10- and 2.53-MeV levels to the ground state and 0.94-MeV level are given in Table VIII on the assumption that the 2.10-MeV level, as well as the 2.53-MeV level, has $J^\pi=2^+$. These strengths were obtained from the lifetime measurements of Litherland *et al.*[10] and our measurements of the branching ratios and mixing parameters. A range of possible values are given for the transitions to the 0.94-MeV level since the mixing parameter was not measured for either the $2.10\rightarrow0.94$ or $2.53\rightarrow0.94$ transition. The predicted strengths[5] of the decay of the lowest 2^+, $T=0$ level of $(2s,1d)^2$ are also given in Table VIII. It is seen that the results for neither level is in violent disagreement with the predictions; but that the 2.10-MeV level gives the best agreement if the $2.10\rightarrow0$ transition has $x=+(3.0\pm0.5)$. If the 3.35-MeV level were the 2^+ level is question then the theoretically predicted intensity ratio for the branches to the ground state and 0.94-MeV level would be $\sim2:1$ while the experimental ratio is $(53\pm5):(4\pm4)$. This is not too strong a disagreement so that the possibility that the 3.35-MeV level is the 2^+ level cannot be eliminated by our present knowledge of the decay of this state.

We conclude that we cannot, on the basis of the available experimental evidence, make a one to one correspondence between the energy levels of F^{18} below 3.5 MeV and the states expected from the $(2s,1d)^2$ configuration. However, one important conclusion seems quite sure and that is that there are at least three and probably four levels below 3.5 MeV which do not belong to the $(2s,1d)^2$ configuration. There are the 1.08-MeV level, either one or another of the two levels at

[49] D. Wilmore (private communication).

[50] S. Hinds and R. Middleton, Proc. Phys. Soc. (London) **A74**, 762 (1959).

[51] We consider agreement within a factor of 2 to be good and within a factor of 4 reasonable.

1.70 or 3.13 MeV, and two out of three of the levels of 2.10, 2.53, and 3.35 MeV.

These additional states presumably arise from the configurations $p^{-1}(2s,1d)^3$ and $p^{-2}(2s,1d)^4$, i.e., to the odd-parity group of states formed by raising one nucleon from the p shell into the $(2s,1d)$ shell, and to the even-parity group of states formed by raising two nucleons from the p shell into the $(2s,1d)$ shell. In other light nuclei, e.g., B^{10}, C^{12}, N^{14}, O^{16}, these two configurations have roughly the same mean energy, and from the systematics it is expected that some of these states will appear below 3.5 MeV in F^{18}. For the odd-parity states at least this statement is supported by the work of Harvey[7] on the $T=1$ spectrum of odd-parity states in mass 18.

It seems clear that considerably more experimental and theoretical work must be done before a reasonably detailed understanding of the F^{18} levels below 3.5 MeV is reached. Of first importance are parity measurements for the 1.08-, 2.10-, 3.13-, and 3.35-MeV levels. By means of these parity determinations, the odd-parity states from the $p^{-1}(2s,1d)^3$ configuration could be isolated and knowledge concerning the degree of mixing of the $(2s,1d)^2$ and $p^{-2}(2s,1d)^4$ configurations could be gained. For instance, if it turns out that these four states all have odd parity then the remaining states should be quite well described by the previous shell-model calculations.[1–5] On the other hand, if it turned out that 3 or 4 of these levels had even parity then a considerable mixing of the two even-parity configurations would be expected and there would be a definite need to extend the theoretical predictions.

VI. ACKNOWLEDGMENTS

We thank Dr. E. Bretscher for the use of the 5-MeV Van de Graaff generator Atomic Energy Research Establishment, Harwell; and we thank T. Sparrow and the operators of the 5-MeV Van de Graaff for their technical assistance. Thanks are due to J. Lowe of Birmingham University for his working out of the lifetime limit for the F^{18} 1.08-MeV level and to A. E. Litherland of Chalk River for a helpful communication on the linear polarization of the F^{18} 0.940-MeV level. D. Wilmore very kindly provided us with some details of his theoretical work on the mass-18 system. Finally, a considerable debt is due Dr. M. A. Grace who initiated the program of which these measurements are a part and who provided many helpful suggestions during the course of this work, and much encouragement.